

DOT/FAA/TCTT-22/30

Federal Aviation Administration
William J. Hughes Technical Center
Aviation Research Division
Atlantic City International Airport
New Jersey 08405

Effect of Active Cargo Containers on Aircraft Smoke Transport

August 2022

Technical Thesis

The research described in this report was funded by the FAA as part of its mission to improve aircraft safety. The views and opinions expressed are those of the author alone and do not necessarily represent the views of the FAA. The FAA assumes no liability for the contents or use thereof. The FAA has not edited or modified the contents of the report in any manner.



U.S. Department of Transportation
Federal Aviation Administration

NOTICE

This document is disseminated under the sponsorship of the U.S. Department of Transportation in the interest of information exchange. The U.S. Government assumes no liability for the contents or use thereof. The U.S. Government does not endorse products or manufacturers. Trade or manufacturers' names appear herein solely because they are considered essential to the objective of this report. The findings and conclusions in this report are those of the author(s) and do not necessarily represent the views of the funding agency. This document does not constitute FAA policy. Consult the FAA sponsoring organization listed on the Technical Documentation page as to its use.

This report is available at the Federal Aviation Administration William J. Hughes Technical Center's Full-Text Technical Reports page: actlibrary.tc.faa.gov in Adobe Acrobat portable document format (PDF).

Form DOT F 1700.7 (8-72)

Reproduction of completed page authorized

| | | | | | |
|--|--|--|--|---|--|
| 1. Report No. DOT/FAA/TCTT-22/30 | | 2. Government Accession No. | | 3. Recipient's Catalog No. | |
| 4. Title and Subtitle Effect of Active Cargo Containers on Aircraft Smoke Transport | | | | 5. Report Date August 2022 | |
| | | | | 6. Performing Organization Code ANG-E21 | |
| 7. Author(s) Andrew Ferraro | | | | 8. Performing Organization Report No. | |
| 9. Performing Organization Name and Address Federal Aviation Administration William J. Hughes Technical Center Aviation Research Division, Fire Safety Branch Atlantic City International Airport, NJ 08405 | | | | 10. Work Unit No. (TRAIS) | |
| | | | | 11. Contract or Grant No. 17-G-006 | |
| 12. Sponsoring Agency Name and Address FAA Northwest Mountain Regional Office 2200 S 216 th St., Des Moines, WA 98198 | | | | 13. Type of Report and Period Covered | |
| | | | | 14. Sponsoring Agency Code AIR-623 | |
| 15. Supplementary Notes Thesis submitted to the School of Graduate Studies, Rutgers, The State University of New Jersey in partial fulfillment of the requirements for the degree of Master of Science Graduate Program in Mechanical and Aerospace Engineering. | | | | | |
| 16. Abstract A simulated model of a full-sized aircraft cargo compartment was used to determine the effect of active cargo containers. Physical testing in conjunction with the simulated cargo compartment was used to validate the accuracy of the Fire Dynamics Simulator model which included an artificial smoke generator. The artificial smoke generator is currently used in certification of smoke detectors in aircraft cargo compartments. It consisted of heaters that vaporize oil to create smoke. Arranging cargo containers with the smoke generator gives a baseline for smoke movement in the compartment. The smoke was measured using lasers and light meters which were partially obscured by the moving smoke. Fans were added to the containers as a stand-in for temperature-controlled cargo containers (TCC), also called "active" cargo containers, that had condenser cooling fans Comparing the experimental test data to the simulated test data showed that the simulation is a good fit. The smoke trends between the tests are very similar and there was a difference in detection time typically less than 10 seconds over the entirety of the tests. Using the Envirotainer RKN e1 as a typical TCC, an airflow of 35 CFM was used for the experimental testing. According to the testing and simulations, using TCCs with airflows of 17.5 or 35 CFM has an inconsistent effect on the smoke detection time, at the extremes, ±20 seconds, ±30% of detection time. At elevated airflow of 70 and 140 CFM, the time to smoke detection was almost always delayed, an average of 30 seconds (+50%) and at most up to 70 seconds (+110%). Delay of smoke detection could cause potentially dangerous conditions in the aircraft. Because of the delay, it is recommended to keep airflow of TCCs to below 70 CFM. | | | | | |
| 17. Key Words Aircraft Fire Safety -- Active Cargo Container Aircraft Fire Safety -- Cargo Fire Aircraft Fire Safety -- Fire Dynamics Simulator Aircraft Fire Safety -- Smoke Detection and Transport | | | | 18. Distribution Statement This document is available to the U.S. public through the National Technical Information Service (NTIS), Springfield, Virginia 22161. This document is also available from the Federal Aviation Administration William J. Hughes Technical Center at actlibrary.tc.faa.gov . | |
| 19. Security Classif. (of this report) Unclassified | | 20. Security Classif. (of this page) Unclassified | | 21. No. of Pages 33 | 19. Security Classif. (of this report) Unclassified |

Effect of Active Cargo Containers on Aircraft Smoke Transport

By

Andrew R Ferraro

A thesis submitted to the

School of Graduate Studies

Rutgers, The State University of New Jersey

In partial fulfillment of the requirements

For the degree of

Master of Science

Graduate Program in Mechanical and Aerospace Engineering

Written under the direction of

Francisco Javier Diez

And approved by

DocuSigned by:
Arnon Marzys
BA79AB2B19D544C...

DocuSigned by:
Richard Hill
68DED067E887420...

DocuSigned by:
Javier Diez
4634F7B041B8430...

New Brunswick, New Jersey

October 2022

ABSTRACT OF THE THESIS

Effect of Active Cargo Containers on Aircraft Smoke Transport

By Andrew R Ferraro

Thesis Director:

Francisco Javier Diez

A simulated model of a full-sized aircraft cargo compartment was used to determine the effect of active cargo containers. Physical testing in conjunction with the simulated cargo compartment was used to validate the accuracy of the Fire Dynamics Simulator model which included an artificial smoke generator. The artificial smoke generator is currently used in certification of smoke detectors in aircraft cargo compartments. It consisted of heaters that vaporize oil to create smoke.

Arranging cargo containers with the smoke generator gives a baseline for smoke movement in the compartment. The smoke was measured using lasers and light meters which were partially obscured by the moving smoke. Fans were added to the containers as a stand-in for temperature-controlled cargo containers (TCC), also called “active” cargo containers, that had condenser cooling fans.

Comparing the experimental test data to the simulated test data showed that the simulation is a good fit. The smoke trends between the tests are very similar and there was a difference in detection time typically less than 10 seconds over the entirety of the tests.

Using the Envirotainer RKN e1 as a typical TCC, an airflow of 35 CFM was used for the experimental testing. According to the testing and simulations, using TCCs with airflows of 17.5 or 35 CFM has an inconsistent effect on the smoke detection time, at the extremes, ± 20 seconds, $\pm 30\%$ of detection time. At elevated airflow of 70 and 140 CFM, the time to smoke detection was almost always delayed, an average of 30 seconds (+50%) and at most up to 70 seconds (+110%). Delay of smoke detection could cause potentially dangerous conditions in the aircraft. Because of the delay, it is recommended to keep airflow of TCCs to below 70 CFM.

TABLE OF CONTENTS

| | Page |
|---|------|
| Effect of Active Cargo Containers on Aircraft Smoke Transport | 1 |
| ABSTRACT OF THE THESIS..... | 2 |
| TABLE OF CONTENTS..... | 4 |
| LIST OF FIGURES..... | 5 |
| LIST OF TABLES..... | 7 |
| LIST OF EQUATIONS | 8 |
| LIST OF ACRONYMS..... | 9 |
| CHAPTERS | 10 |
| Introduction | 10 |
| Previous Results | 10 |
| Altitude Chamber | 11 |
| FDS Model Validation | 12 |
| Experimental Setup | 16 |
| Container Layout..... | 17 |
| Laser Setup..... | 20 |
| DC-10 FDS Model..... | 21 |
| Smoke Detectors | 24 |
| Experimentation and Validation | 24 |
| Results..... | 27 |
| Simulated Results | 27 |
| Experimental Results | 30 |
| Smoke Detector Comparison | 32 |
| Experimental vs Simulation | 33 |
| Temperature Controlled Containers | 38 |
| Maximum Airflow..... | 41 |
| Conclusion..... | 46 |
| Future Work | 47 |
| APPENDIX..... | 49 |
| REFERENCES..... | 57 |

LIST OF FIGURES

| | Page |
|--|------|
| Figure 1: Altitude chamber experimental test setup (Karp, 2019)..... | 12 |
| Figure 2: Smoke generator cut-away modeled in FDS..... | 13 |
| Figure 3: Altitude chamber test in FDS | 14 |
| Figure 4: LD3 Container..... | 17 |
| Figure 5: Envirotainer RKN e1 (Envirotainer, 2021)..... | 18 |
| Figure 6: Mock TCC | 19 |
| Figure 7: DC-10 test cell layout..... | 20 |
| Figure 8: DC-10 mid compartment with smoke generator and lasers | 21 |
| Figure 9: Simulated model of DC-10 mid cargo compartment | 23 |
| Figure 10: Test 1 simulated results | 28 |
| Figure 11: Test 1 velocity slice | 29 |
| Figure 12: Test 2 simulated model..... | 29 |
| Figure 13: Test 2L simulated results | 30 |
| Figure 14: Test 1 experimental results..... | 31 |
| Figure 15: Test 1, four runs of meter H..... | 32 |
| Figure 16: Test 1 experimental vs simulated..... | 34 |
| Figure 17: Test 2L experimental vs simulated results..... | 34 |
| Figure 18: Test 1 time difference and error between test methods | 35 |
| Figure 19: Test 1 obscuration difference and error between test methods..... | 36 |
| Figure 20: 10% criteria for simulated results | 37 |
| Figure 21: Smoke detection time at 10% obscuration..... | 38 |

| | |
|---|----|
| Figure 22: Compartment filled with LD3s vs TCCs | 39 |
| Figure 23: Simulation 2L vs 2A | 39 |
| Figure 24: Simulation 6L vs 6A | 40 |
| Figure 25: Difference in detection time between TCC and LD3 runs | 41 |
| Figure 26: Test 2 varied TCC airflow | 42 |
| Figure 27: Test 2 varied TCC airflow time difference..... | 43 |
| Figure 28: Test 4 varied TCC airflow time difference..... | 43 |
| Figure 29: Test 6 varied TCC airflow time difference..... | 44 |
| Figure 30: Test 8 varied TCC airflow time difference..... | 45 |
| Figure 31: Percent time difference with varied TCC airflow for tests 2, 4, 6, and 8 | 46 |

LIST OF TABLES

| | Page |
|--|------|
| Table 1: Smoke Generator Properties..... | 15 |
| Table 2: Test matrix..... | 26 |

LIST OF EQUATIONS

| | Page |
|---|------|
| Equation 1: Beer-Lambert law (Ramachadran, 2018)..... | 24 |

LIST OF ACRONYMS

| Acronym | Meaning |
|---------|--|
| TCC | Temperature Controlled Container |
| FAA | Federal Aviation Administration |
| FDS | Fire Dynamic Simulator |
| LD3 | Unit Load Device, IATA designation AKE |

CHAPTERS

Introduction

Smoke detection in aircraft is a critical safety feature which keeps crew and passengers safe and aircraft in operation. It is important to understand any possible changes in the performance of the smoke detection system. Cargo containers with a refrigeration cycle are now available to fly critical pharmaceuticals and other high value products. These containers keep their contents cold, while fans on the exterior cool a condenser. With the addition of cooling fans on these cargo containers, there is the possibility of an effect on the airflow pattern in a cargo compartment. This report seeks to measure and quantify any effect of those changes.

Previous Results

FAA report AR-09-52 titled “Effects of Cargo Loading and Active Containers on Aircraft Cargo Compartment Smoke Detection” (Blake, 2014) had a series of tests to determine the effect of active cargo containers on smoke detection time in a Boeing 727 aft cargo compartment. Blake used a series of physical tests with a mix of standard and active cargo containers. Smoke detection was directly measured by a forced air detection system with multiple ports along the compartment ceiling. His tests had multiple arrangements of containers and directions of fans. The result of that investigation was “active containers did not have a consistent influence on smoke detection times under the airflow conditions tested”

The tests that Blake ran were very applicable to the specific setup of each test but did not reveal how the airflow was affected or the path of the smoke in the compartment. Using smoke

detectors only gives a signal of off or on, but no measurement of the amount of smoke passing it. These shortcomings are some of the considerations that went into the experimental design of the testing conducted for this report.

Altitude Chamber

A series of experiments were conducted in a chamber called the altitude chamber. The altitude chamber consists of a large box which is approximately 6'x8'x6'. The chamber can be completely sealed to control the environment, including pressure. During these tests the internal pressure was ambient. The experimental setup for the altitude chamber tests consisted of a smoke generator and laser obscuration meters. The smoke generator was the Concept Smoke Detector Testing system (SDT) which used a heating element to evaporate oil vapor. The oil used in the smoke generator was a proprietary mineral oil mixture manufactured by Concept, called Smoke Oil 180. Lasers and laser power meters were used together to create an obscuration meter. These were mounted to a rack horizontally at six-inch intervals above the smoke generator's chimney, as seen in Figure 1. Spacing between the laser diode and laser power meter was four feet. (Karp, 2019)



Figure 1: Altitude chamber experimental test setup (Karp, 2019)

FDS Model Validation

The altitude chamber tests were used as validation for the model built in Fire Dynamic Simulator (FDS). The model was created to-scale with the chamber, lasers obscuration meters, and smoke generator. The smoke generator was disassembled and measured precisely so that it could be represented in the simulation accurately. Due to the voxelated nature of the FDS scripting language, features such as rounded or circular holes were modeled as pixelated shapes. A cutaway of the smoke generator modeled in FDS can be seen in Figure 2.

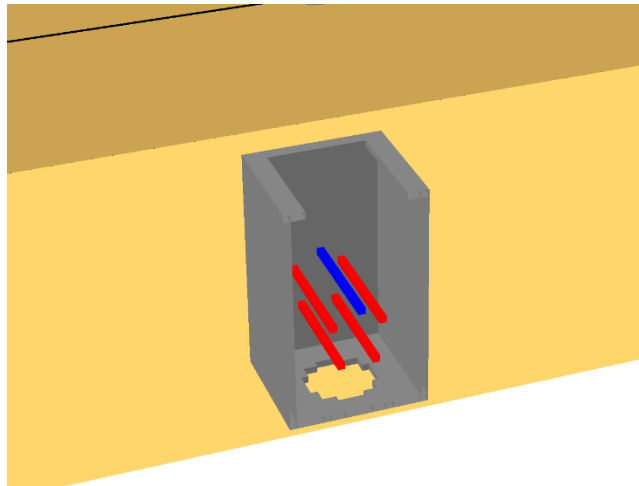


Figure 2: Smoke generator cut-away modeled in FDS

The physical smoke generator consisted of a chimney with vapor nozzle, and oil reservoir with control electronics. For the sake of simplicity, only the chimney was modeled in FDS. The chimney was eight by eight inches by 16 inches tall. There was a gap of a half inch underneath the chimney that allowed for airflow into the hole at the bottom. The chimney and oil reservoir can be seen in entirety at the bottom of Figure 1. Oil was introduced to the chimney by pressurizing the oil reservoir with compressed inert gas. This forced the oil up the internal plumbing to the heat exchanger.

The smoke generator had two types of electric heaters. The first type of heater was the heat exchanger for the oil vapor. The heat exchanger was preheated to 315°C where the oil would be instantly vaporized. Attached to the heat exchange was a nozzle which dispersed the oil vapor into the top of the chimney. To model this, a solid bar with smoke emitters on each side was placed at the height of the nozzle and spanned the width of the chimney, shown in blue above.

The second type of heater is shown as the red bars. These were approximately half inch round resistive heater bars, which spanned the entire eight-inch width. The chimney and heaters created strong convection currents which were the main driver of airflow in the system. All four chimney heaters had a power of $640W$ which corresponded in FDS to heat flux of $14.22 kW/m^2$.

The altitude chamber itself was modeled as a perfectly sealed box which was approximately six by eight feet wide and six feet tall. There was no ventilation or interior fans added. The laser obscuration meters were modeled as a built-in feature of FDS. They were massless devices that spanned four feet in the same setup as the altitude chamber physical tests.

Figure 3 shows a cross section of the whole setup modeled in FDS while smoke was being generated.

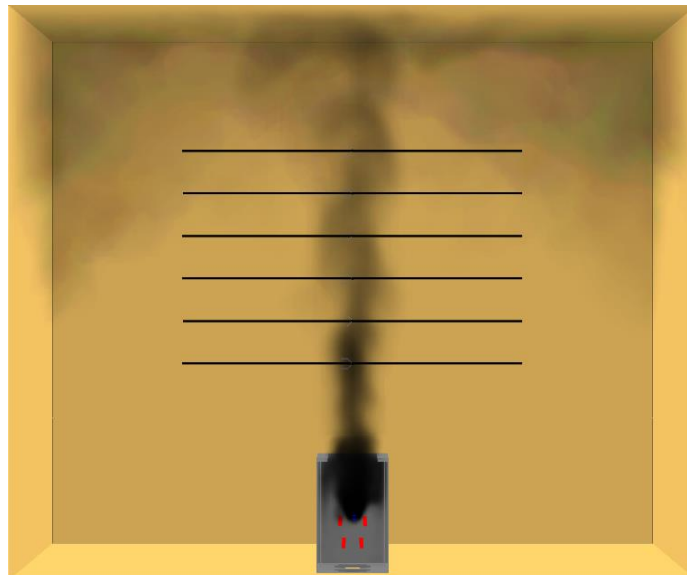


Figure 3: Altitude chamber test in FDS

FDS is primarily used for fire testing, hence the name. In this simulation, the smoke generating surface was defined as a particle emitter instead of a chemical burner. FDS is a suitable simulation environment to use with a particle emitter and convection currents utilizing its large eddy simulation process.

Since Concept was unable to provide all of the exact chemical properties of the smoke oil, some of the properties had to be gathered from similar mineral oils. The final parameters of the oil and smoke emitter are tabulated below.

| Property | Value | Unit |
|--|--------------|-------------|
| Mass Extinction Coefficient | 2600 | unitless |
| Density (liquid oil) | 845 | kg/m^3 |
| Specific Heat (liquid oil) | 1.67 | $kJ/kg * K$ |
| Vaporization Temperature | 430 | $^{\circ}C$ |
| Melting Temperature | -30 | $^{\circ}C$ |
| Enthalpy of Formation | -400 | kJ/mol |
| Heat of Vaporization | 977 | kJ/kg |
| Heat of Vaporization Reference Temperature | 316 | $^{\circ}C$ |
| Viscosity (liquid oil) | 0.0026 | $kg/m * s$ |
| Conductivity (liquid oil) | 0.136 | $W/m * K$ |
| Beta (liquid oil) | 0.00098 | $1/K$ |
| Initial Temperature | 315 | $^{\circ}C$ |
| Particle Diameter | 0.2 | μm |

Table 1: Smoke Generator Properties

Mass Extinction Coefficient was experimentally determined by matching the laser obscuration percentage to the altitude chamber experimental test with the same liquid oil flow rate.

Density, vaporization temperature, and particle diameter came from the Concept documentation for the smoke oil (Concept SDT). The rest of the values were required for the

particle system to work but were not critical values. They were obtained from typical mineral oil properties from The Engineering Toolbox (The Engineering Toolbox, 2001).

Experimental Setup

Testing for the LD3 to TCC comparison would be both simulated and conducted physically. Like the altitude chamber tests, the physical testing would help to validate the simulated results. A modified DC-10 cargo aircraft located in the Full-Scale Fire Test Facility of the FAA's William J. Hughes Technical Center was selected as the test cell. It was chosen because the mid cargo compartment was in good condition and easily accessible for the necessary testing equipment. The Full-Scale Fire Test Facility was also a completely enclosed testing facility which was air conditioned and heated, making it more consistent during testing.

The Concept SDT smoke generator was again used for this test. To be able to use the same FDS model as the altitude chamber experiment, the same settings on the smoke generator were used. All four 160W chimney heaters were enabled, totaling 640W and the heat exchanger was set to 315°C. The oil in the smoke generator was pushed into the heat exchanger by pressurized inert gas. Since the chimney heaters create the convection current, the speed of the smoke exiting the chimney is only dependent on the heater power and not the gas pressure. In certification tests, typical gas pressure is 10 – 26psig. There was no prescribed amount of gas to use since a higher pressure would just make more smoke. 2.5psig of nitrogen gas was used in this experiment. That amount was chosen by trial and error in order to record the laser obscuration meters without the power level dropping to 0W, effectively running out of measurement range.

The laser power meters were zeroed before the start of each day's tests and the 0W point was used as 100% obscuration. Before adding any smoke, the lasers were turned on and the unobstructed laser measurement was used as the 0% obscuration reading. Each laser has a different 0 – 100% range so they are calculated individually using linear interpolation. The unobstructed laser had a power of 2 – 4mW.

Container Layout

The DC-10's mid cargo compartment was large enough to hold about 20 LD3 containers. To reduce the size of the testing area, plastic sheeting was used to block off both sides of a section that measured 260", which could hold exactly eight LD3 containers side by side. An eight-container area was chosen so that there would be enough variation in the number of arrangements of containers but not increase the simulation computation time unnecessarily.

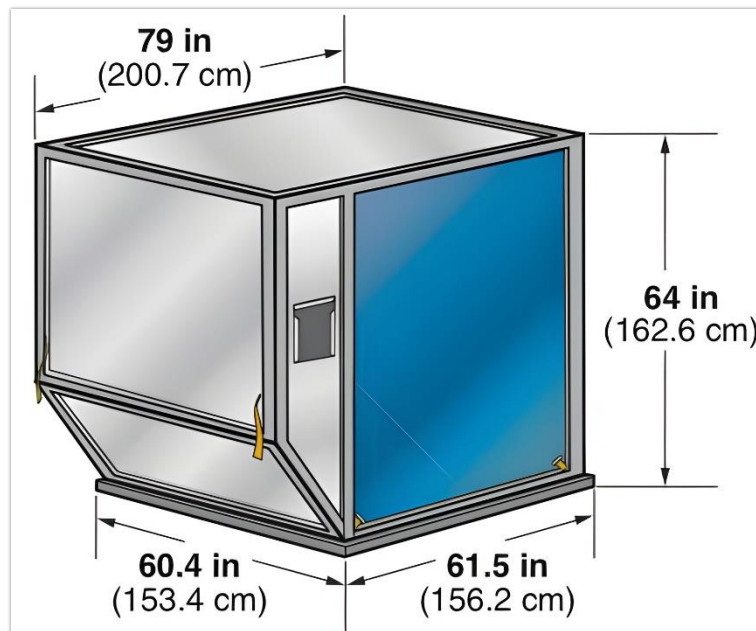


Figure 4: LD3 Container

The containers used were standard LD3 size containers with canvas doors such as in Figure 4. There was no modification to those containers. The mock TCCs used in this experiment were modeled after the Envirotainer “RKN e1” temperature-controlled containers, shown in Figure 5. Roof exhaust (1) has an airflow of 35.4 *CFM*. Exhaust/inlet (2) has a combined airflow of 4 *CFM* which is low enough to ignore for simplicity. Inlet (3) is the source of air for the system (Envirotainer, 2021).

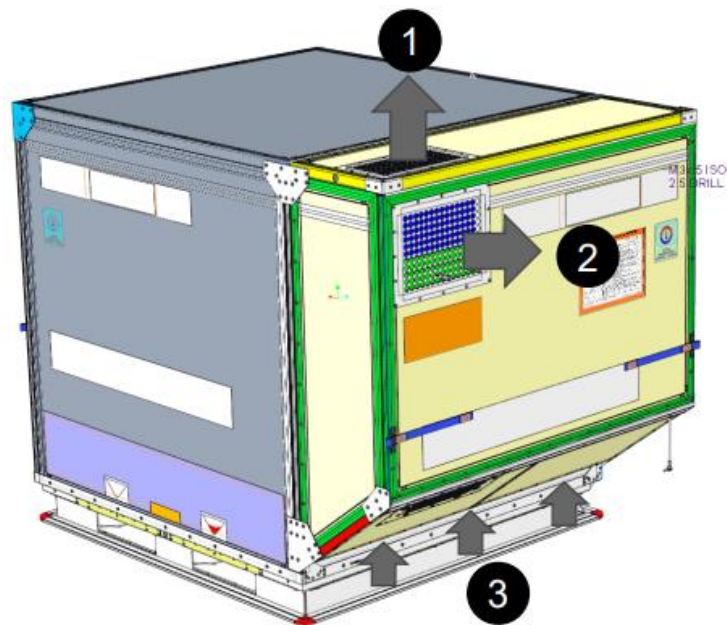


Figure 5: Envirotainer RKN e1 (Envirotainer, 2021)

The mock TCCs were built from all metal LD3 containers and modified with fans. As can be seen below, a 144 *mm* computer fan was added to ducting at the top of the container. Not shown is the intake vent in the bottom angled side. The airflow was measured with a cone anemometer and the voltage of the fan was adjusted to 14.9 *V*, which matched the airflow to exhaust (1).

Two of these mock TCCs were built. This allowed for testing in enough of the test cases to compare the results to the simulations.



Figure 6: Mock TCC

The containers fit in the compartment with about five inches of gap between them. This was measured before each new test setup for consistency. Eight positions were used for the containers and each test had containers only at these locations. The smoke generator, however, was either placed in the center of a position, or in-between two of the positions. The arrangement of each container position is shown below.

Obscuration Meters

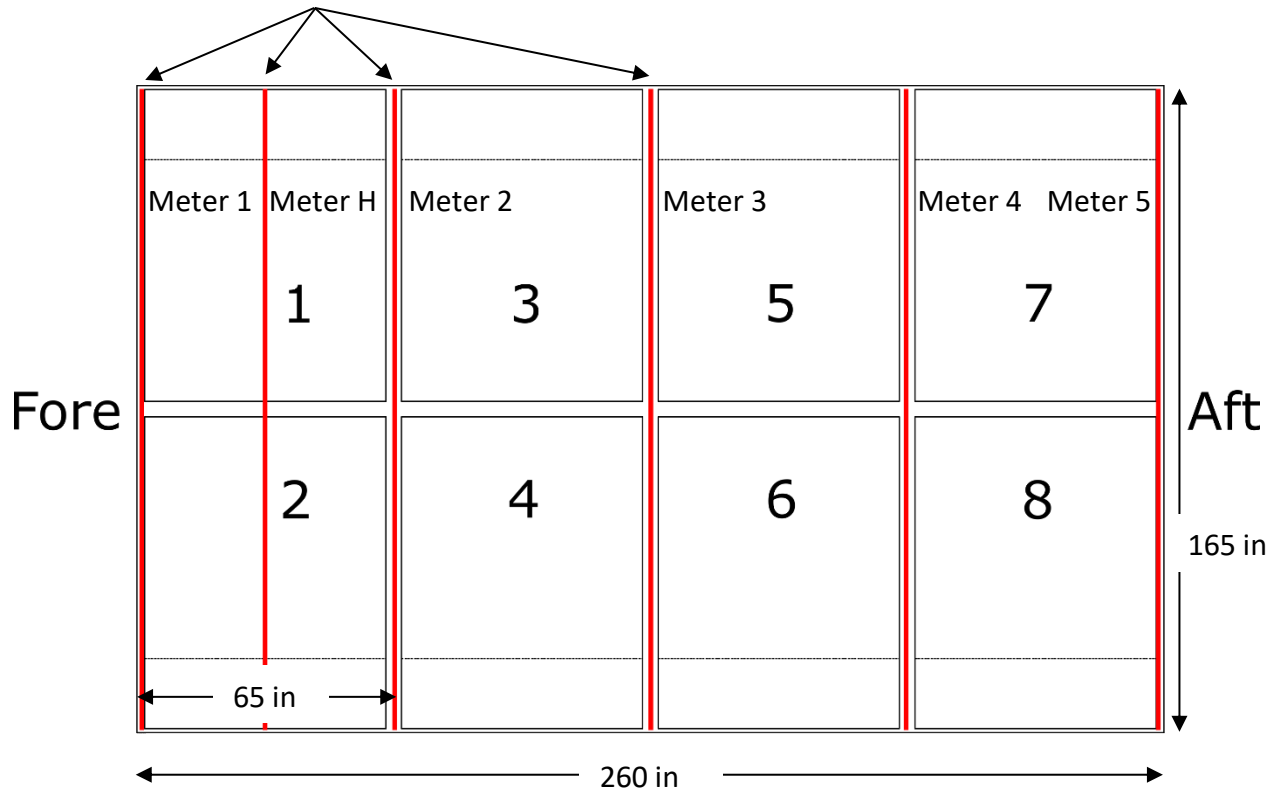


Figure 7: DC-10 test cell layout

Laser Setup

Six laser obscuration meters spanned the whole width of the test cell. Meters 1 and 5 are located in the fore and aft corners of the compartment. Meters 2-4 are evenly spaced between them, at 65-inch increments. An additional meter was placed above the smoke generator, between positions one and two. Each obscuration meter consisted of a laser emitter and a laser power meter which output a reading in Watts. The lasers power meters recorded to the testing computer on the PowerMaxPC software. The recording software recorded readings once per second.

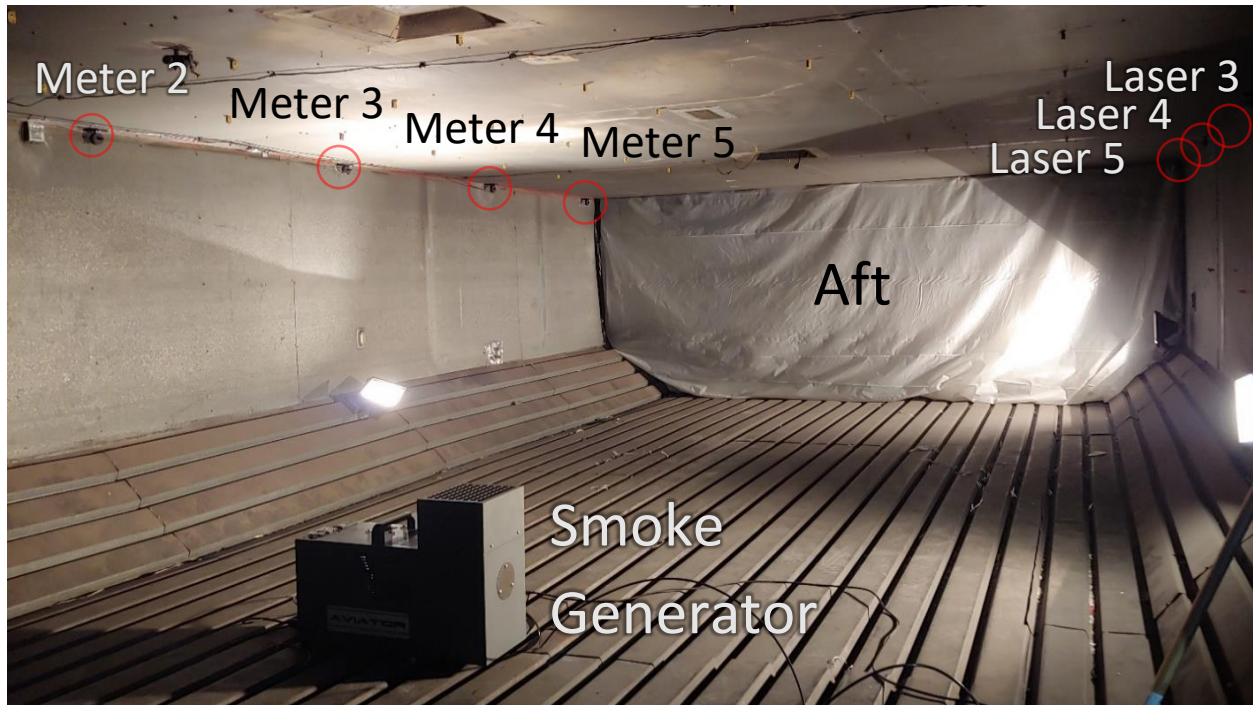


Figure 8: DC-10 mid compartment with smoke generator and lasers

Figure 8 shows a view of the inside of the DC-10 mid compartment looking towards the aft of the aircraft. Several of the lasers and laser power meters can be seen attached to the ceiling, circled in red. In the center of the compartment is the Concept smoke generator positioned between locations one and two. The halogen lamps were later removed due to the heat creating other air currents.

DC-10 FDS Model

The smoke generator model was applied to the lower cargo compartment of the DC-10 modeled in FDS. The cargo compartment and containers were designed using Blender mesh modeling software and voxelized using an FDS plugin. The design was based on measurements from the LD3 containers on site that would be used for the physical testing. The LD3 containers

had a square base that extended at a 45° angle on one side to match the shape of the cargo compartment. The TCC used the same model as the LD3 but included vents in the top and bottom. The intake vent stretched across the sloped side near the bottom of the container, about four inches from the floor. The exhaust vent of the TCC was located on the top face of the container, near one of the corners. There was about four inches between the ceiling of the compartment and the top of the containers. The DC-10 model was based on measurements from the physical test cell. The slotted floor was not represented in the FDS model.

The smoke generator from the altitude chamber model was placed into the simulated DC-10 compartment. Since the model was validated in the altitude chamber testing, no changes had to be made. The smoke generator could be easily moved to any LD3 position in the DC-10.

Like the altitude chamber model, the laser obscuration meters used the built-in FDS function. The meters were positioned as shown in Figure 7. Five lasers were positioned between each LD3 location labeled from one to five, from fore to aft. An extra laser was placed above positions one and two and labeled H, for heat. A gap of two inches was left on all sides of the lasers from any obstructions. The model with no cargo containers installed is shown below; the smoke generator is placed between positions one and two.

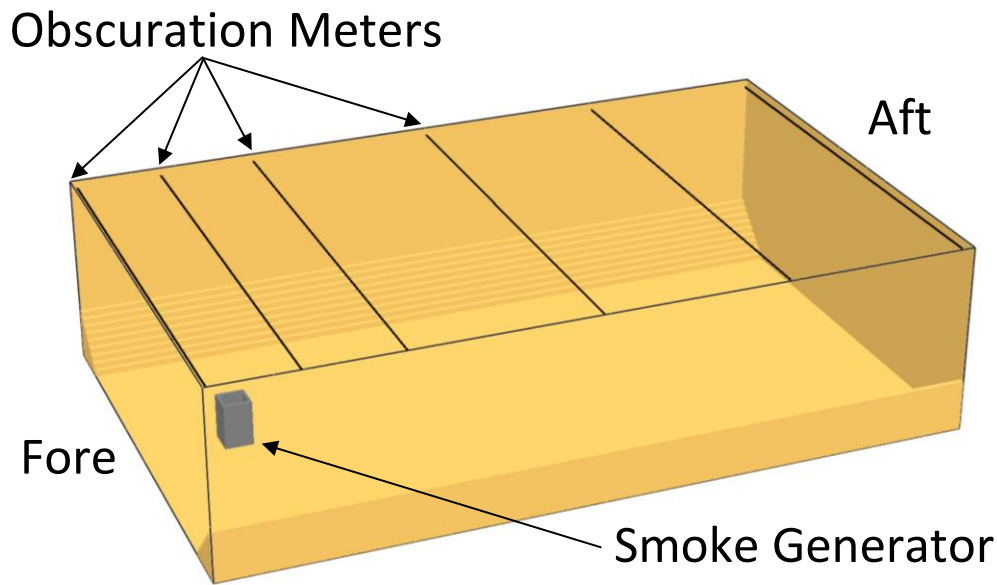


Figure 9: Simulated model of DC-10 mid cargo compartment

The resolution of most of the simulation mesh was $0.05m$ which is approximately two inches. Convergence testing was conducted to ensure that the mesh was fine enough. It is possible that a larger resolution would work for the compartment, but it was kept small so that there would be enough cells between the containers and walls. The mesh transitioned to $0.025m$ around the smoke generator area, then went to $0.0125m$ containing the smoke generator itself. This was necessary to have an accurate airflow around the heaters and chimney since the gaps and heaters were small. Convection was the main driving force of the air flow so that change was critical. The airflow around the base of the chimney had specific testing comparing different mesh resolution and spacing of the chimney to the floor. The gap between the compartment and the top of the containers was similarly tested and was deemed sufficient for the simulation.

Smoke Detectors

In order to compare the laser readings to a real-world aircraft cargo compartment, an array of smoke detectors were installed in the ceiling. They were placed along the centerline of the compartment, above meters one, three, and five. The smoke detectors were not a permanent addition, once a baseline was taken for comparison, they were all removed.

The detectors used were Meggitt model 602 and had an alarm threshold of 94-96% light transmission per foot (Meggitt, 2021). This value cannot be directly compared to obscuration over the cargo compartment so the equivalent obscuration can be calculated using the Beer-Lambert law below. By using the width of the compartment at 13.5 ft, 94-96% light transmission per foot is equivalent to 42-57% light obscuration over the entire width.

$$\frac{I}{I_0} = 10^{-ad}$$
$$\log_{10} \frac{I}{I_0} = -ad$$

I = Incoming intensity
 I_0 = Exiting intensity
 a = Mass extinction coefficient
 d = Distance

Equation 1: Beer-Lambert law (Ramachadran, 2018)

Experimentation and Validation

The test plan consisted of 10 test cases organized in Table 2. The first was a completely empty compartment with the smoke generator between positions 1 and 2. This would become a baseline while calibrating the laser obscuration meters and choosing the nitrogen gas pressure for the smoke generator. The next nine test cases include a case “L” and “A” which are for LD3 and Active container, respectively. All test cases were simulated using FDS, but not all could be

run physically. Most of the “L” tests were run physically, with a few removed to save time. Any “A” case with only two TCCs were run physically since only two mock TCCs were built.

| Test | Smoke Generator Location | Cargo Containers | | | | Test Type |
|-----------------------|--------------------------|------------------|-----|-----|-----|-----------------------|
| | | 1 | 3 | 5 | 7 | |
| | | 2 | 4 | 6 | 8 | |
| 1 - Empty Compartment | Between location 1 and 2 | SG | | | | Simulated Physical |
| | | | | | | |
| 2 L | Between location 1 and 2 | SG | LD3 | | | Simulated Physical |
| | | | LD3 | | | |
| 2 A | Between location 1 and 2 | SG | TCC | | | Simulated Physical |
| | | | TCC | | | |
| 3 L | Between location 1 and 2 | SG | | LD3 | | Simulated Physical |
| | | | | LD3 | | |
| 3 A | Between location 1 and 2 | SG | | TCC | | Simulated Physical |
| | | | | TCC | | |
| 4 L | Between location 1 and 2 | SG | | | LD3 | Simulated Physical |
| | | | | | LD3 | |
| 4 A | Between location 1 and 2 | SG | | | TCC | Simulated Physical |
| | | | | | TCC | |
| 5 L | Between location 1 and 2 | SG | LD3 | LD3 | | Simulated Physical |
| | | | LD3 | LD3 | | |
| 5 A | Between location 1 and 2 | SG | TCC | TCC | | Simulated |
| | | | TCC | TCC | | |
| 6 L | Between location 1 and 2 | SG | LD3 | LD3 | LD3 | Simulated Physical |
| | | | LD3 | LD3 | LD3 | |
| 6 A | Between location 1 and 2 | SG | TCC | TCC | TCC | Simulated |
| | | | TCC | TCC | TCC | |
| 7 L | Between location 1 and 2 | SG | | LD3 | LD3 | Simulated Physical |
| | | | | LD3 | LD3 | |
| 7 A | Between location 1 and 2 | SG | | TCC | TCC | Simulated |
| | | | | TCC | TCC | |
| 8 L | Location 2 | LD3 | LD3 | LD3 | LD3 | Simulated |
| | | SG | LD3 | LD3 | LD3 | |

| | | | | | | |
|------|------------|-----|-----|-----|-----|-----------|
| 8 A | Location 2 | TCC | TCC | TCC | TCC | Simulated |
| | | SG | TCC | TCC | TCC | |
| 9 L | Location 2 | LD3 | LD3 | LD3 | LD3 | Simulated |
| | | SG | | | | |
| 9 A | Location 2 | TCC | TCC | TCC | TCC | Simulated |
| | | SG | | | | |
| 10 L | Location 1 | SG | LD3 | LD3 | LD3 | Simulated |
| | | | | | | |
| 10 A | Location 1 | SG | TCC | TCC | TCC | Simulated |
| | | | | | | |

Table 2: Test matrix

For the physical testing inside the DC-10, each test setup was run three to six times. Before each run, a series of checks were done to confirm the starting laser readings were correct, the nitrogen pressure regulator was set, any TCC fans were powered, and the smoke generator heaters were all on and up to temperature. To start each run, the smoke was triggered remotely while the pressure regulator was monitored for any changes. After 60 seconds, the smoke was switched off and another 240 second timer was set to complete the test.

After each test run, the compartment was opened up and fans were added to blow out the smoke that accumulated. After the smoke was removed, the compartment was left to sit for five minutes to let the air settle after being blown around. This also let the convection current from the chimney heater to develop since the chimney heaters stayed powered on throughout each test day.

To ensure proper circulation of the air inside the compartment, the simulated tests were run for 300 seconds with full chimney heater power, then the smoke oil was introduced for 60

seconds. After the remaining 240 seconds, the test was complete. Since these tests were done in FDS, there was no variation between tests with identical parameters, so each test case only had to be run once.

Results

Simulated Results

The simulation results show a clear flow of the smoke from the generator towards the aft of the compartment, and back towards the fore end. The belief is that the heat from the smoke generator's heater establishes a circulating current in the top section of the compartment. In tests with containers, those containers disrupt the air circulation or create other air patterns. Figure 10 is a graph of each obscuration meter over time. Meter H is always the first meter to register the smoke because it is directly above the smoke generator. Meters 1 through 5 are evenly spaced from fore to aft every 65" in the compartment and typically see smoke in that order.

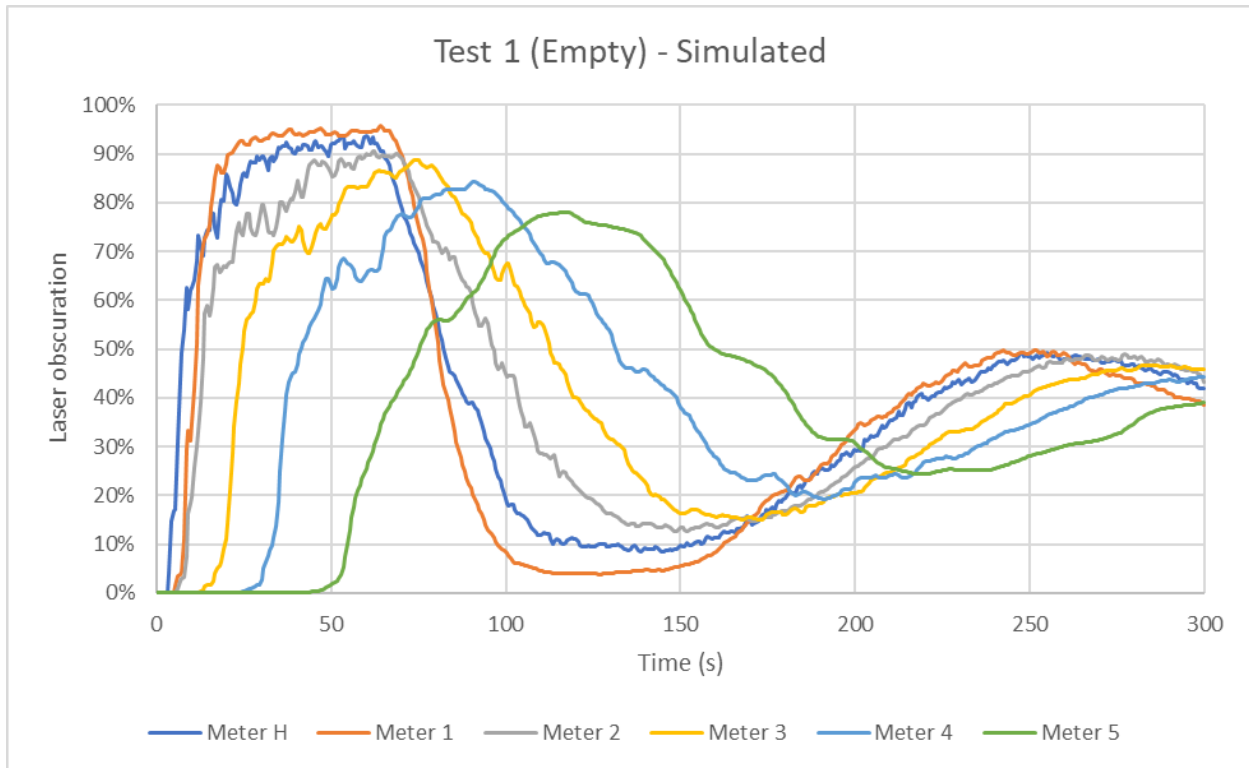


Figure 10: Test 1 simulated results

The peaks of the meters are about 60 seconds long which correspond with the 60 seconds of smoke generation. The closer to the smoke generator the meter was, the longer and flatter the plateau of the graph. After the 60 seconds of smoke generation, there is a sharp drop off to very low obscuration, 5-25%. Then, the smoke circulates around the entire compartment and can be seen on the meters again, this time in order of 1, H, then 2 to 5, which is the order they are positioned fore to aft as laid out in Figure 7. The cycle of the circulation is approximately 200 seconds and a velocity slice of test 1 is shown below. There is a fast-moving plume out of the smoke generator, shown in green. The slower moving currents are shown in light blue. The smoke moves towards the aft of the container along the ceiling but moves towards the fore-end about two feet below the ceiling.

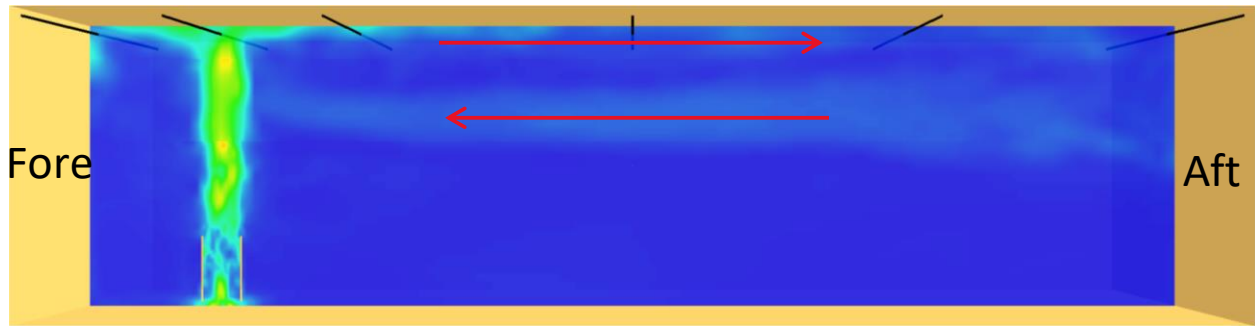


Figure 11: Test 1 velocity slice

There is a 300 second pre-smoke time that is not shown in the results. During this time, the smoke generator heaters are enabled at full power, but smoke is not added. This gives more than enough time for the convection currents to be established. The heaters stay on at full power for the duration of the test.

Test 2 has a much different shape compared to test 1. There are two containers next to the smoke generator which separate the compartment into two areas. Neither of these areas have enough space or convection to create substantial circulating currents. The simulated model of test 2 is shown in Figure 12.

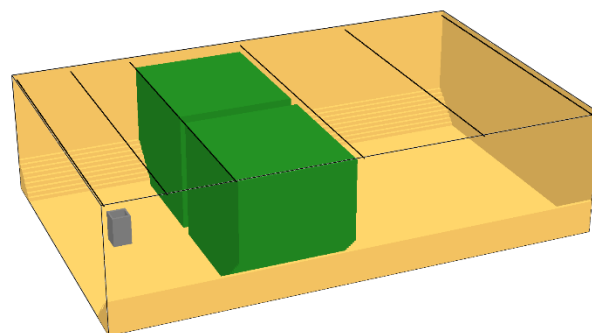


Figure 12: Test 2 simulated model

In Figure 13, this is evident where after the 60 seconds of smoke generation, the obscuration percentage settles to the steady state instead of oscillating. The other tests have similar, or a combination of these effects. The complete set of results is included in the appendix.

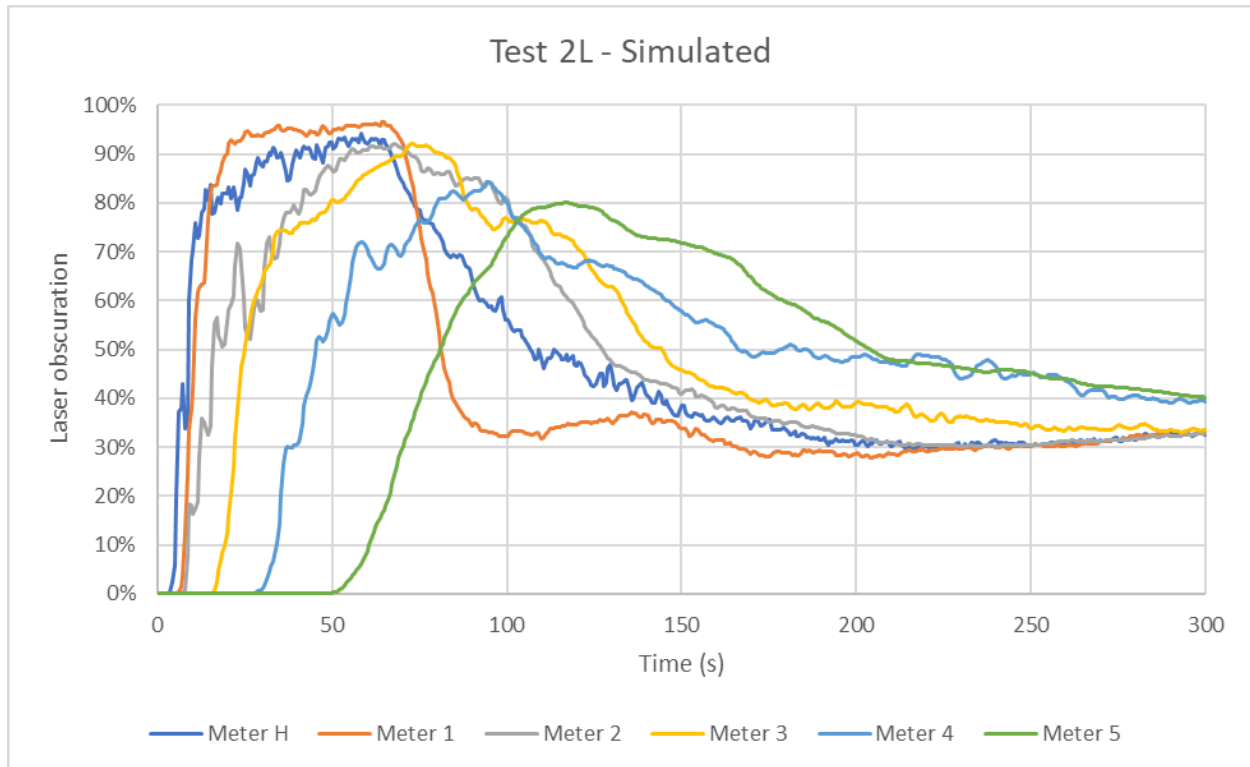


Figure 13: Test 2L simulated results

Experimental Results

Each experimental test was repeated between three to six times and processed in Excel, a total of around 80 individual test runs were conducted. The results are aligned based on the first activation of meter H for each run, then they are averaged together. Test 1 is shown in Figure 14. There was a small dip in obscuration as the nitrogen pressure achieved steady state in the

lines. The dip did not have any significant impact on the results since the bulk of the smoke was still being generated.

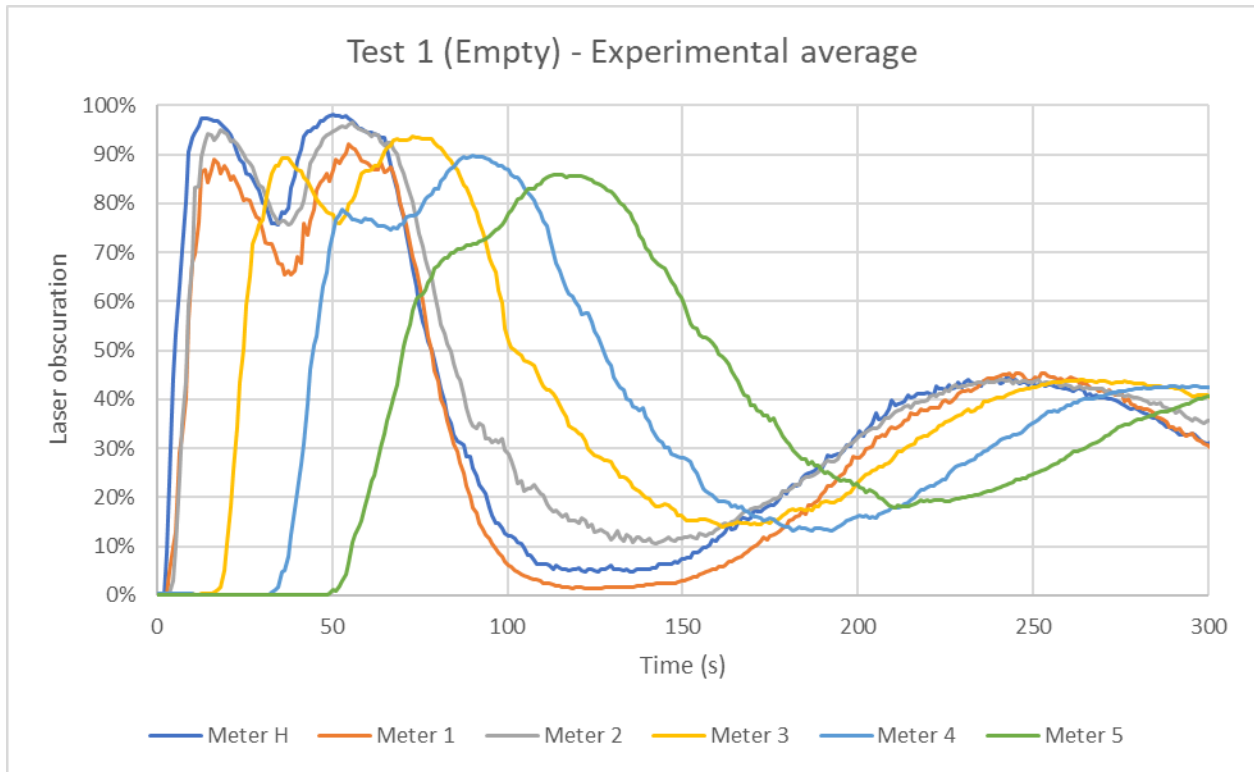


Figure 14: Test 1 experimental results

Figure 15 shows the output of meter H for the six runs from test 1. The test runs are consistent with each other and have similar time periods. The times from each peak of obscuration to trough of smoke reduction to peak of circulation are all within a few seconds. The obscuration percentage is also very repeatable with the bulk of the variation due to unknown variables including sensor noise, inconsistent aerosol, and environmental changes such as temperature and humidity.

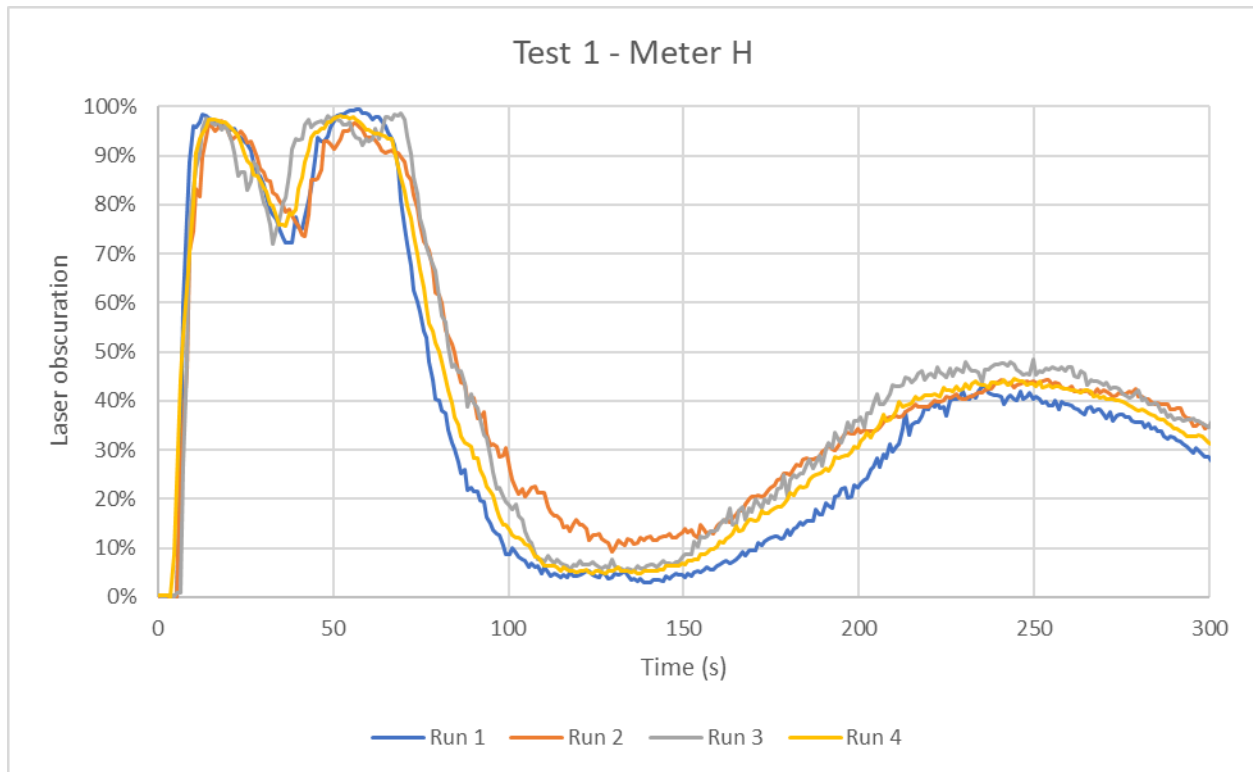


Figure 15: Test 1, four runs of meter H

Smoke Detector Comparison

The results of the smoke detector tests showed varied detection obscuration. It ranged from around 30% to over 100% obscuration. Some of the variation could be explained by the increased delay associated with an enclosed detector compared to the instantaneous laser power meters. An additional reason for this could be the fact that the laser spans a long distance and creates an average reading, while the smoke detector is a point measurement.

In certification tests, a higher pressure yielding more smoke is used. The pressure was reduced for this study to preserve the measurable range of the laser power meters without clipping the measurements at 100% obscuration. For these reasons, it was determined appropriate to

choose an obscuration criterion of 10%. In most tests, 10% is where the laser obscuration meters started to have a measurable reading but before the readings plateau. In later results, the 10% criterion is used as a way to consolidate the tests into concise and comparable values.

Experimental vs Simulation

Comparing the experimental tests to the simulated tests shows a very close trend. Using comparisons of a few select test setups, the similarity can be seen below. Figure 16 shows test case 1 with the experimental and simulated results. Only meters 1, 3, and 5 are shown for clarity. For the first 200 seconds, the graphs are extremely similar and only vary by noise or small time shift. Towards the later section of the tests, some drift in the obscuration percentage can be seen. The FAA's certification of smoke detection typically require detection within 60 seconds; considering the chaotic nature of fluid simulations, this is a satisfactory result.

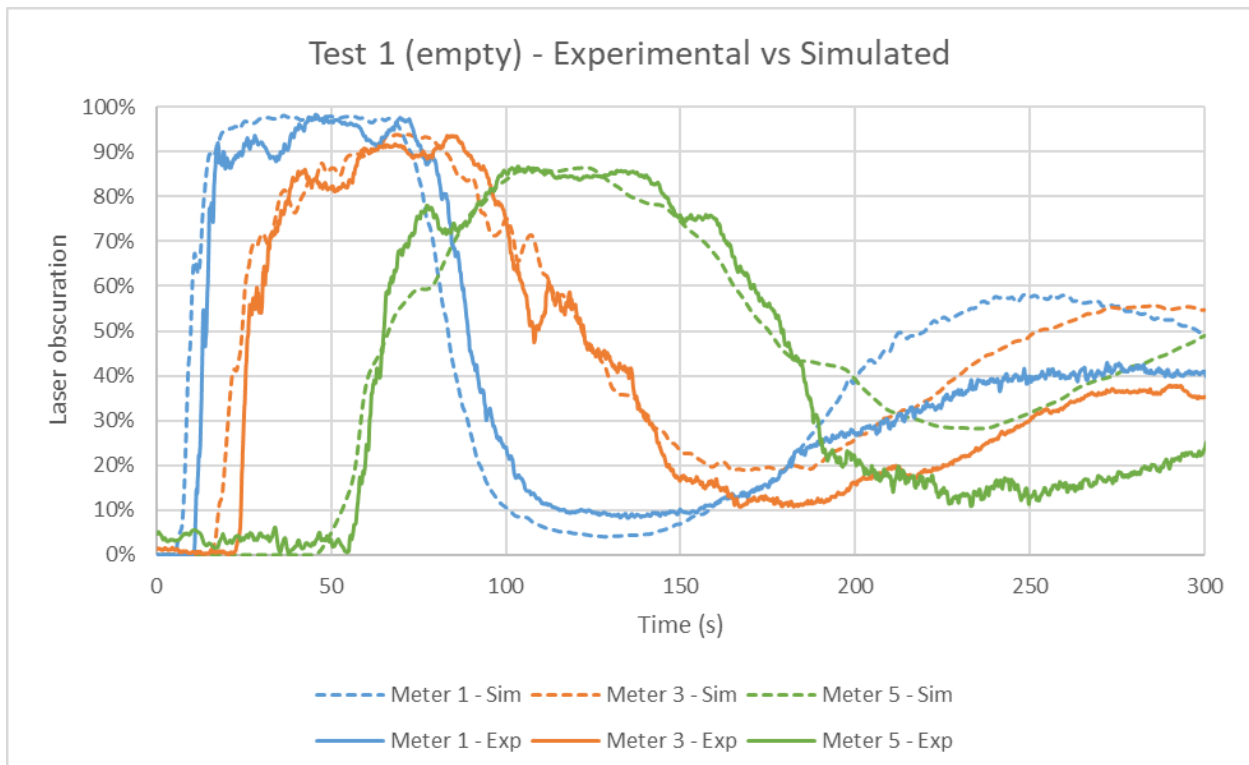


Figure 16: Test 1 experimental vs simulated

below is the same graph for test case 2L. There is a similar level of correlation as from test 1. The shapes of the experimental and simulated results are very close to each other. The laser obscuration drifts apart towards the second half of the graph. This could be due to the increased complexity of the test when adding cargo containers. As always, the most important section of the results is within the first 60 seconds.

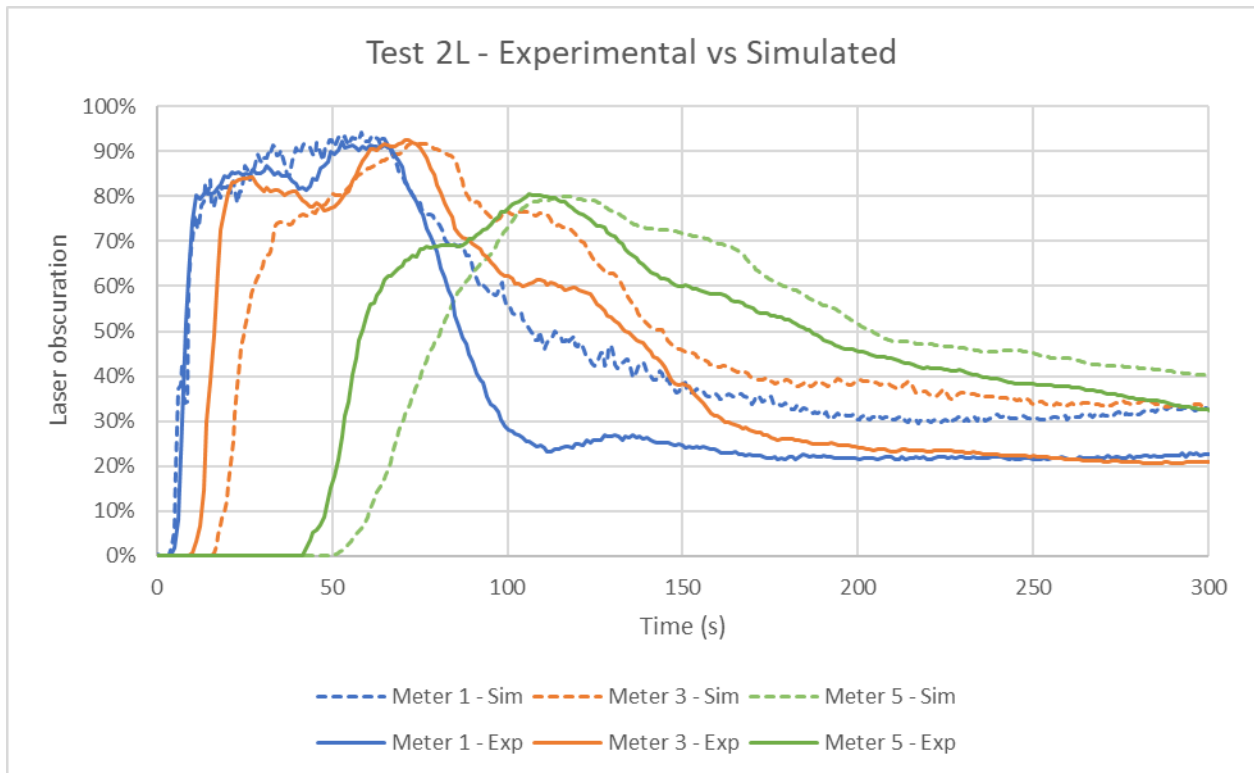


Figure 17: Test 2L experimental vs simulated results

One way to quantify the differences between the experimental and simulated tests is by comparing the peaks and troughs of the graphs. The time difference in Figure 18 is obtained by finding the peak obscuration time of meter H and subtracting it from the time of the lowest

obscuration of each meter. To calculate percent error, the physical test is considered the control. This shows the timescale accuracy of the simulation over time. It can be seen that the error does not increase over the later meters in Test 1 and the percent error is below 7%.

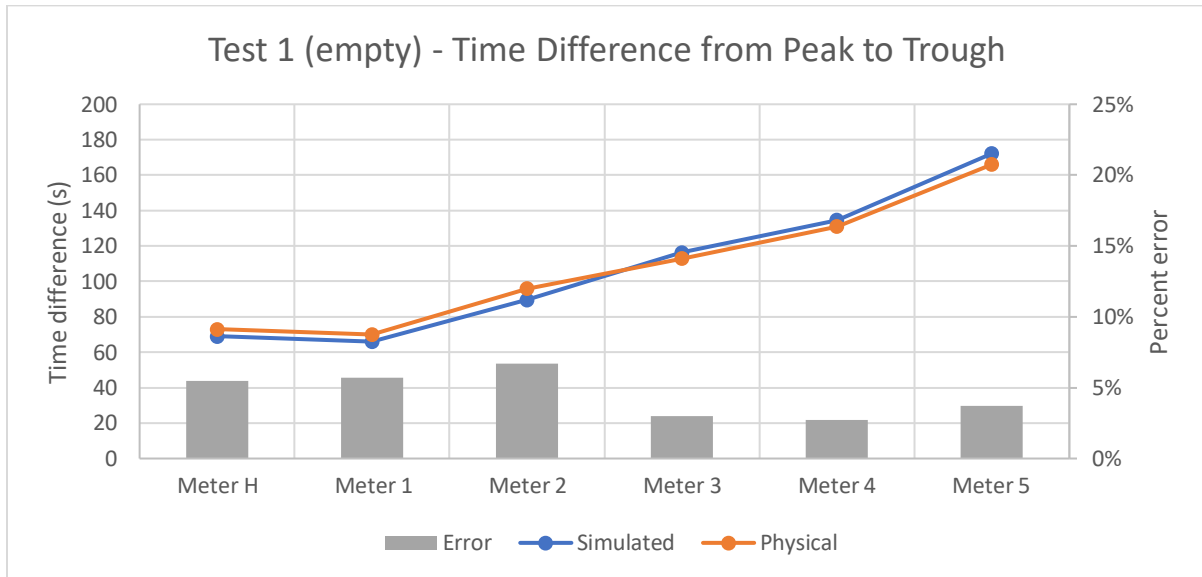


Figure 18: Test 1 time difference and error between test methods

The obscuration difference in Figure 19 is obtained by taking the same points as the time difference chart above. From the chart, it can be seen that the simulated tests have a smaller obscuration drop compared to the experimental tests during the latter half of the test. The first four simulated meters all read within 10% of the experimental meters, while the last two reach a maximum error of 18%. These results are due to the simulation not being able to match the smoke dispersion of the experimental tests. This issue is only apparent later in the tests.

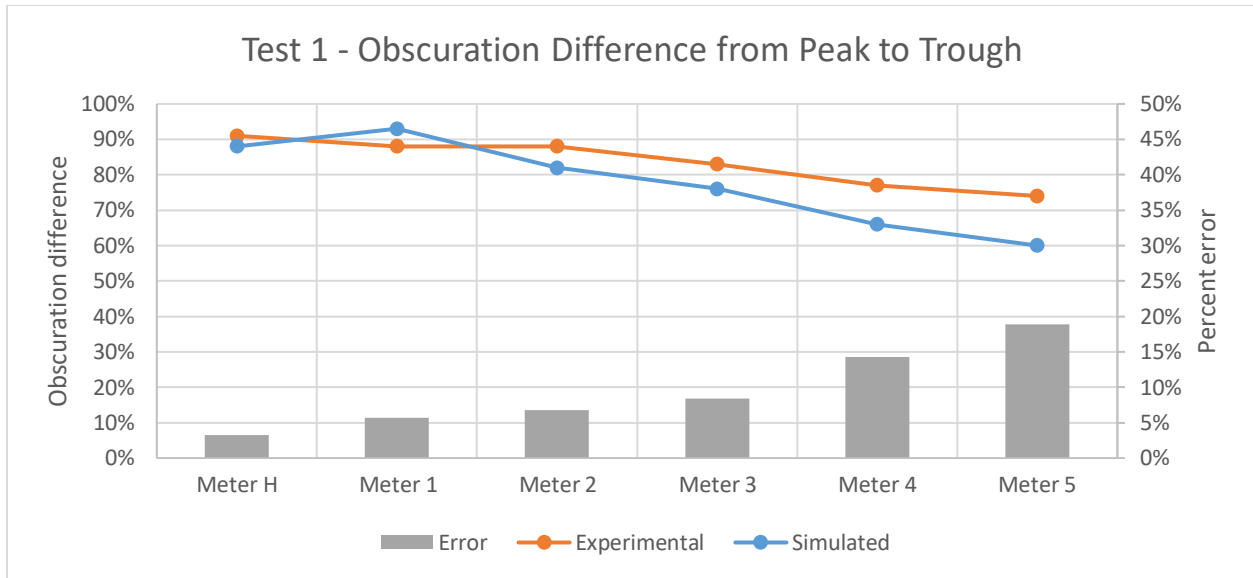


Figure 19: Test 1 obscuration difference and error between test methods

The peak to trough comparison was used on test 1 due to the obvious periodic circulation of the smoke. This movement is not consistent in the rest of the test cases and most cases cannot be evaluated this way. For the remainder of the tests, the 10% smoke detection criterion is used. Figure 20 shows the simulated tests 1 through 7, which all have a corresponding experimental test. The solid lines are all LD3 tests while the dashed lines are all TCC tests. These tests all follow the same general shape, and no outliers are visible.

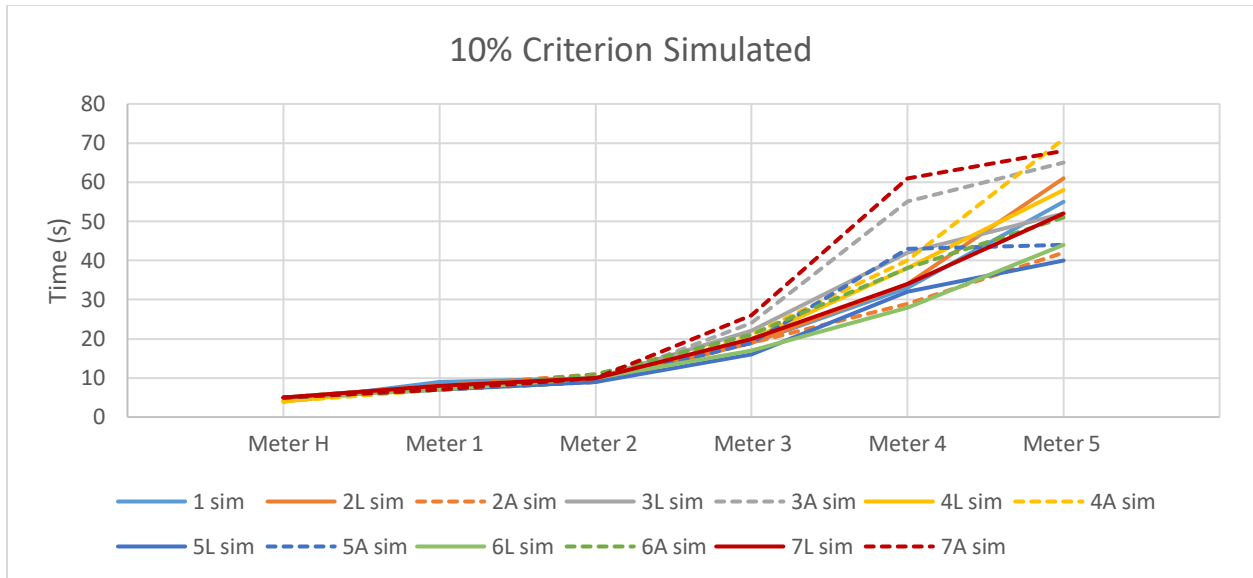


Figure 20: 10% criteria for simulated results

Comparing those simulated tests to the experimental tests gives Figure 21. Here, the experimental time was subtracted from the simulated time. Positive time difference means that the simulated test reached 10% obscuration sooner than the experimental test. Negative time difference means that the experimental test reached 10% obscuration sooner. There were abnormalities in the 3A and 4A comparison that led to large outliers, these have been removed from the data. Those tests both had compounding differences which caused the last meters to translate badly in this specific criterion. The general trend is that the simulated tests reached 10% obscuration sooner than the experimental tests. The difference is only a few seconds though, and the average ranges from less than a second at meter H to about five seconds at meter 5.

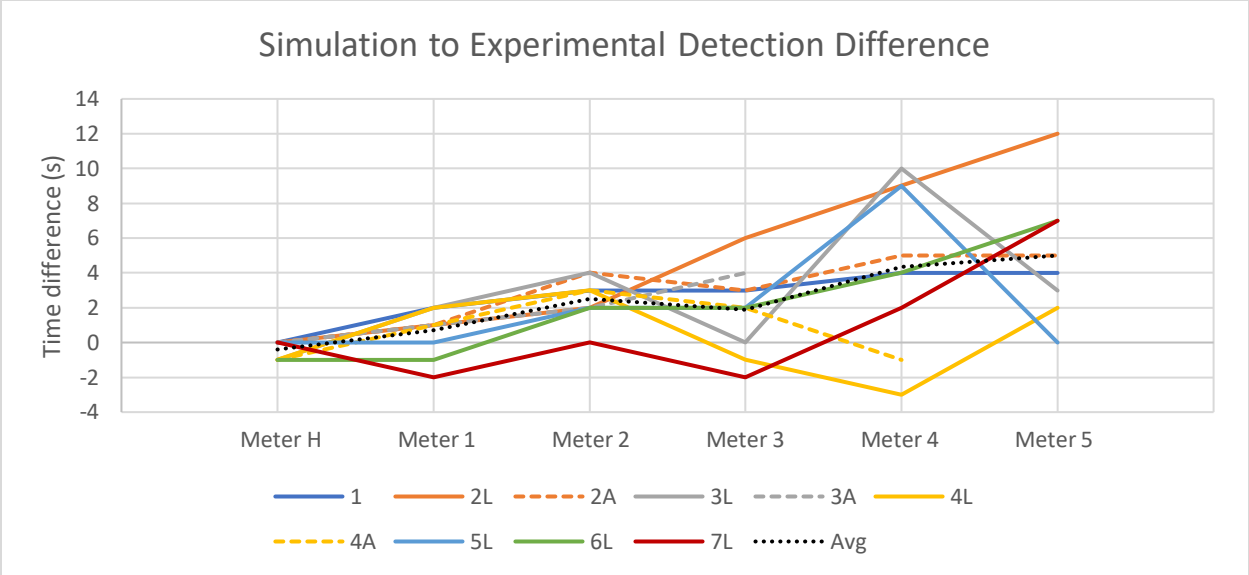


Figure 21: Smoke detection time at 10% obscuration

Temperature Controlled Containers

The temperature-controlled container tests were simulated for each test case. All LD3s in each test case were replaced with TCCs, there were no tests with LD3s and TCCs mixed. Figure 22 shows test 6 with LD3s on the left, and on the right, replaced with TCCs. The LD3s and TCCs are the same size in the simulation. The lower intake vents of the TCCs are not visible behind the compartment wall. Since only two mock TCCs were created, they were only used in test cases with two containers, those were test cases 2, 3, and 4.

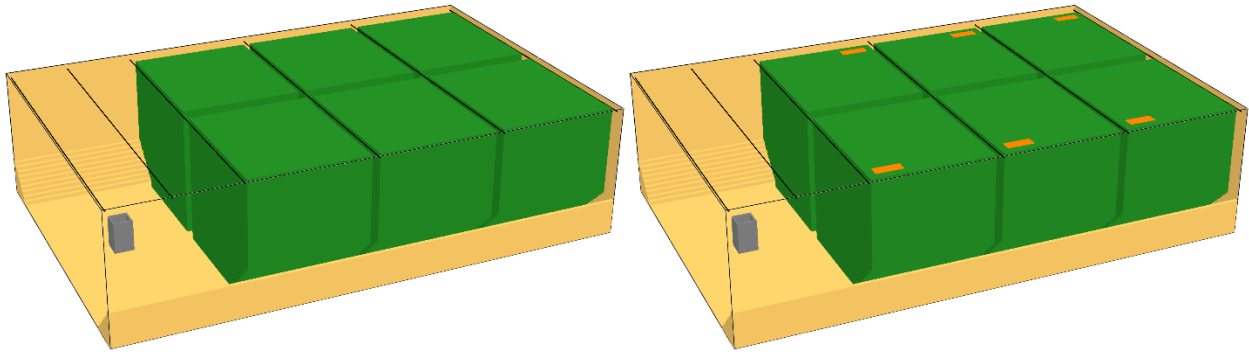


Figure 22: Compartment filled with LD3s vs TCCs

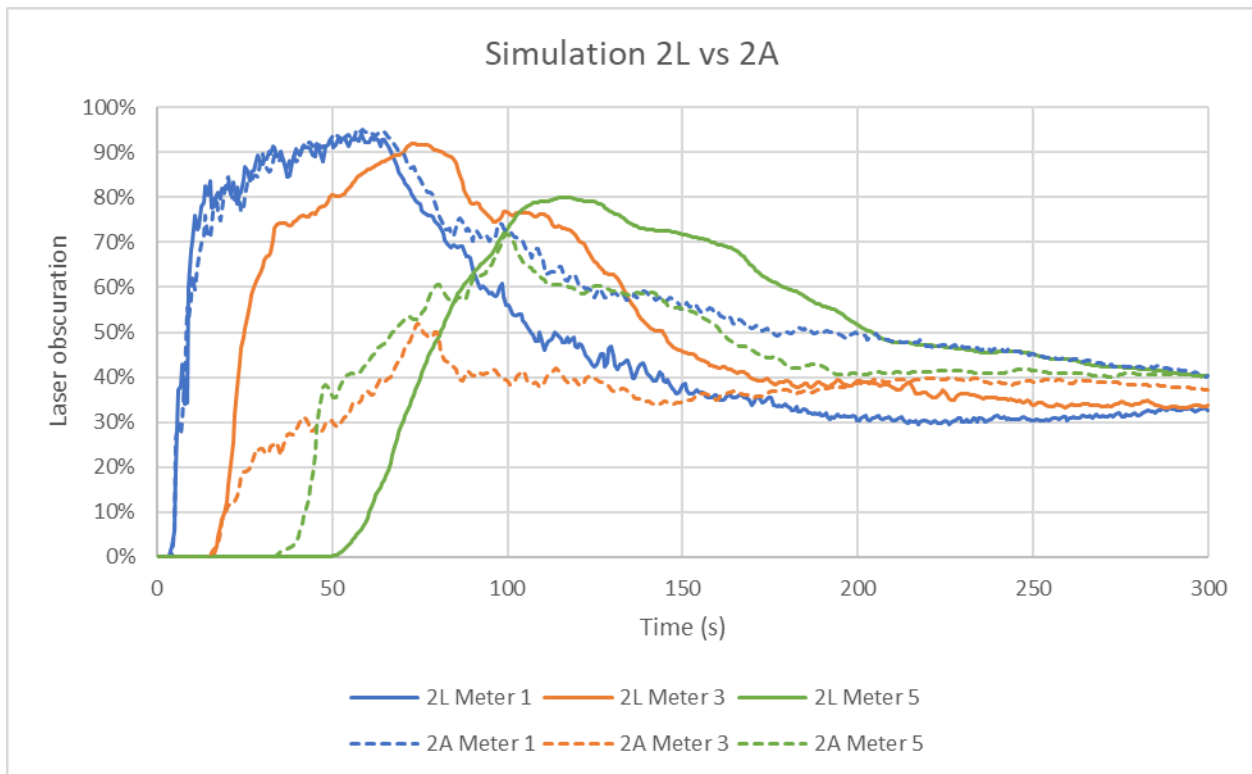


Figure 23: Simulation 2L vs 2A

Figure 23 shows the difference between the LD3s and TCCs for test case 2. The containers sit between meters 2 and 3. The meters further than the containers from the smoke generator detect much less smoke on the TCC run than the LD3 run. Even so, meter 5 detects smoke

earlier on the TCC run than the LD3 run. Meter 1 is mostly the same in the first 100 seconds but does not drop in obscuration as much in the TCC run. This means that the TCCs were preventing the smoke from moving past them. Figure 24 showing test 6 has a similar conclusion. The one difference is that meters 3 and 5 detect smoke slightly later with TCCs.

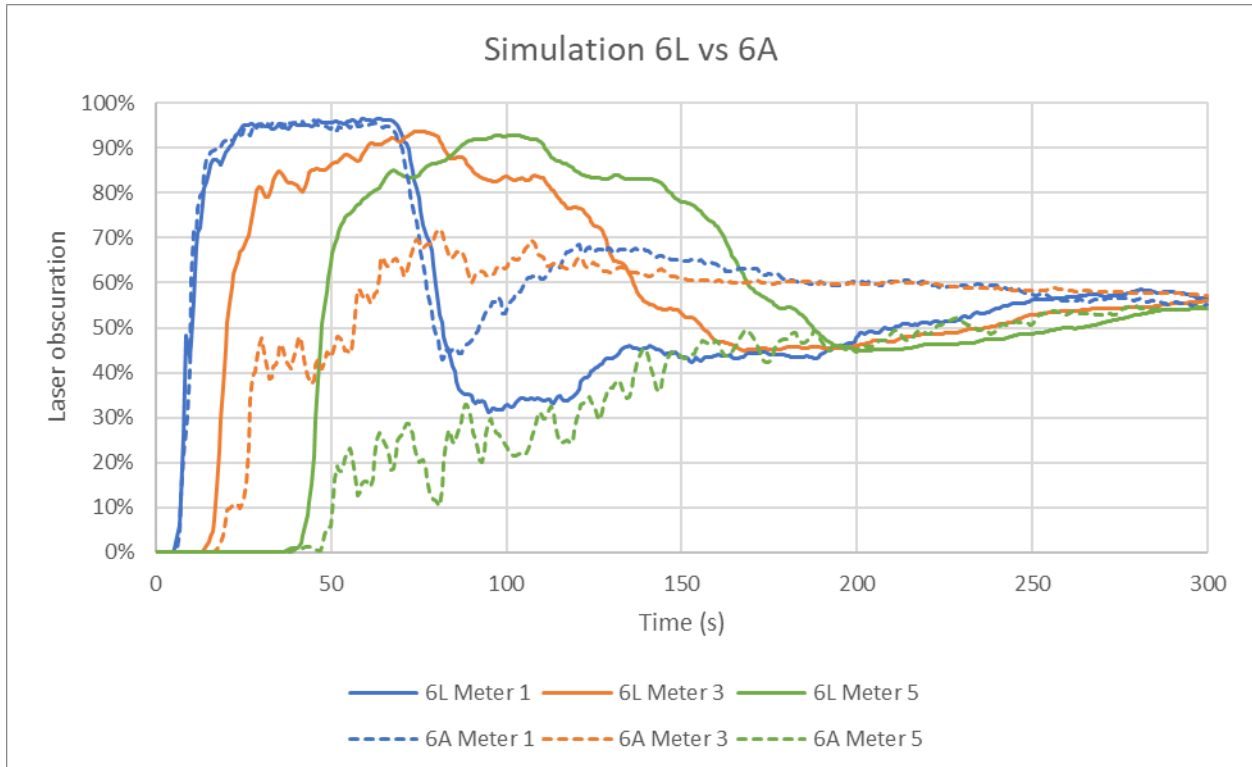


Figure 24: Simulation 6L vs 6A

Figure 25 shows the normalized difference in detection time between the LD3 and the TCC runs. The TCC time was subtracted from the LD3 time; a negative time difference means that the TCC caused the smoke detection sooner, and a positive time difference means that the TCC delayed the smoke detection. This was done to compare the TCC runs directly to the corresponding LD3 runs and not to a baseline like test 1, with no containers.

Tests 2 and 8 are outliers in this chart. From studying the simulation replay, this is by chance. In some test cases, the air current develops in such a way that the smoke is propelled faster than without the TCC fans. There is no trend that is apparent from these tests that points to a configuration causing those currents. It is worth noting that the number of containers did not have a general increase in time difference. Tests two, three, and four all had two containers. Tests five, seven, nine and ten had three or four containers. Tests six and eight had six or seven containers. The change in time is more dependent on the specific container layout.

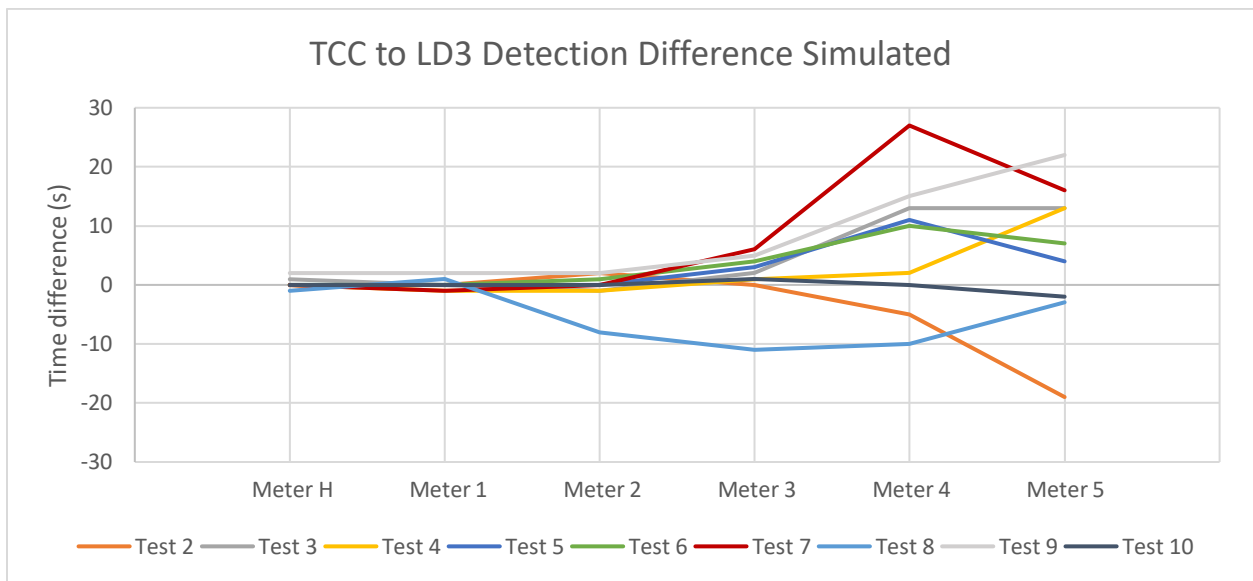


Figure 25: Difference in detection time between TCC and LD3 runs

Maximum Airflow

Determining the maximum airflow of a temperature-controlled container can be done by considering each arrangement of containers and varying the airflow. With the established model for smoke generation and detection, this can be accomplished easily. below can be seen

a comparison of different container fan speeds for test 2's configuration. Test 2L is the control with no fans and 2A is the documented 35 CFM from Envirotainer.

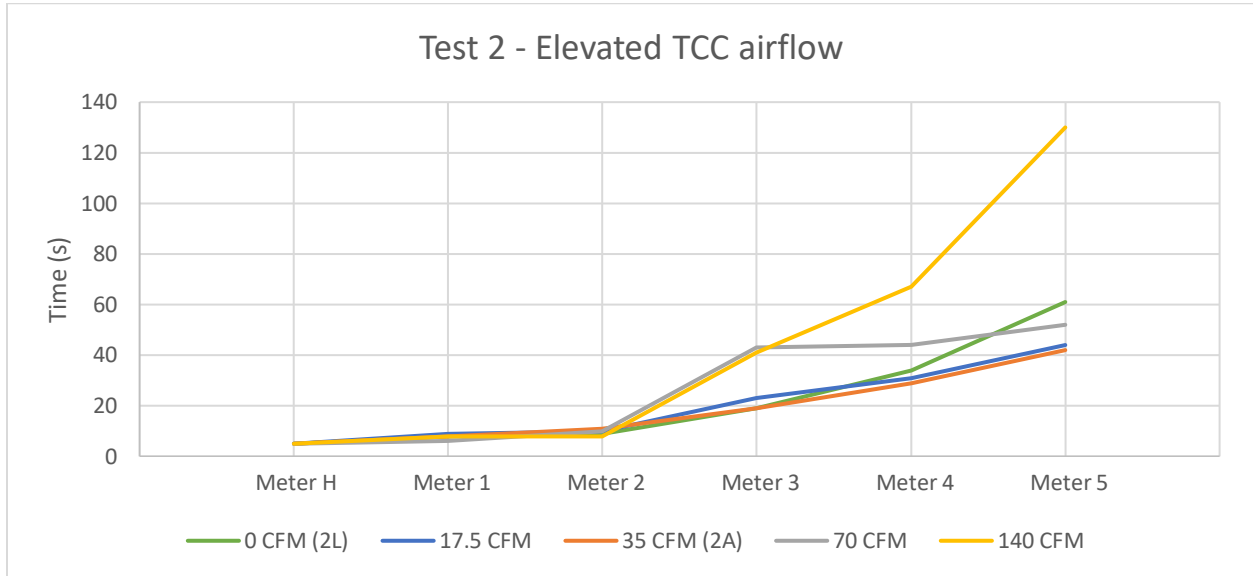


Figure 26: Test 2 varied TCC airflow

Subtracting test 2L (0 CFM) from each test with airflow, the difference is shown in Figure 27. 17.5 CFM and 35 CFM (2A) have a minimal change compared to the 2L baseline. Only towards meters 4 and 5 a substantial negative time difference occurs which corresponds to those tests reaching 10% obscuration faster than the baseline. In the 70 CFM run, there is a large delay in meters 3 and 4 while the others don't change much. In the 140 CFM runs however, meters 3 to 5 show a very large time difference and is around double the detection time.

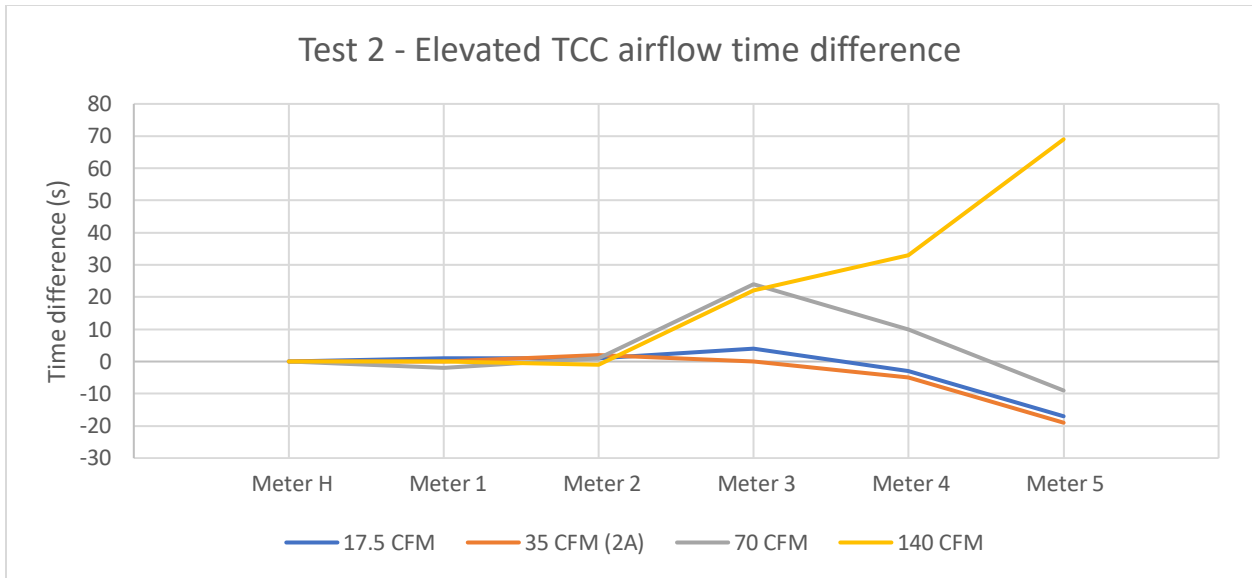


Figure 27: Test 2 varied TCC airflow time difference

Figure 28 shows the time difference in test case 4. The trend of time difference in test 4 is very different from that of test 2. With the containers towards the aft of the compartment in test 4, there is simple correlation of higher airflow leads to longer detection time.

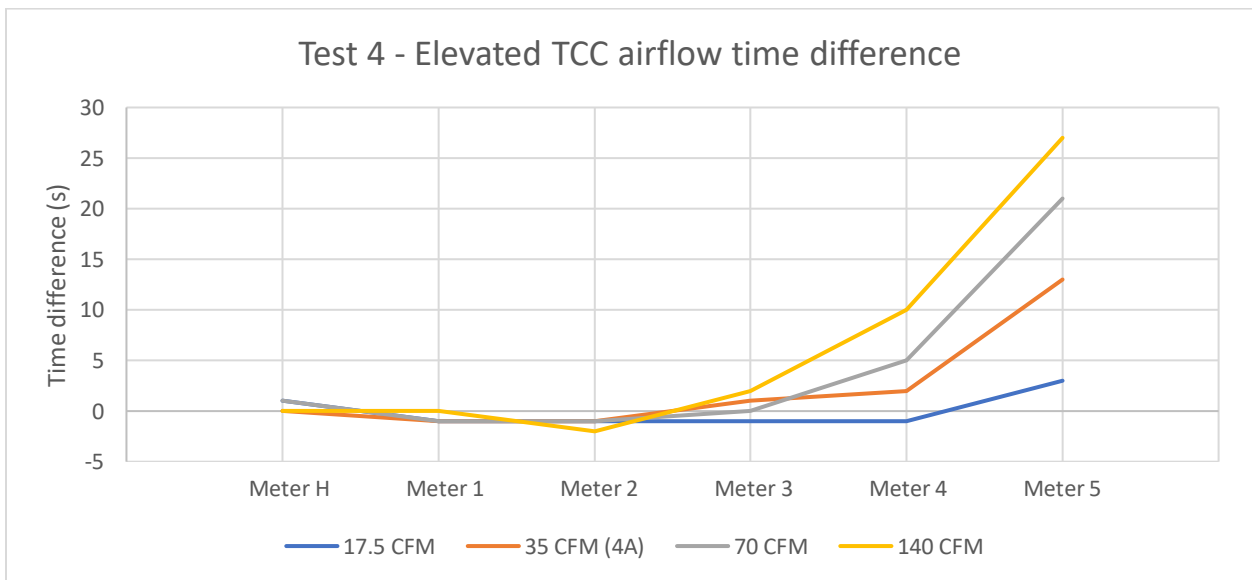


Figure 28: Test 4 varied TCC airflow time difference

Figure 29 showing test 6's time difference again shows a different trend. This test with six containers has a general increase in detection time with increased airflow, however the curve of the time difference is different of that in test 4.

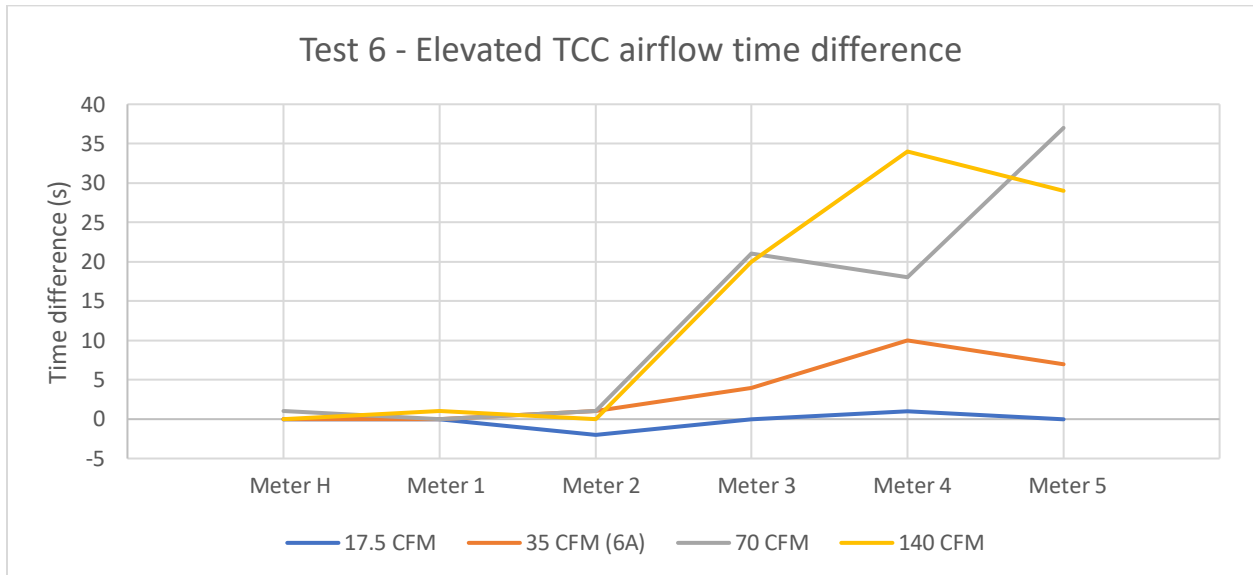


Figure 29: Test 6 varied TCC airflow time difference

Test 8 only has one additional container compared to test 6. Figure 30 shows a similar but distinctly different trend to test 6. The last three meters show a comparable increase in detection time but to a lesser extent. The test 8 setup has the smoke generator offset from the center of the container and has an uneven number of containers. With the TCCs moving the air around, a vortex forms around the smoke generator. This is likely the reason for the first few obscuration meters to have a different trend than those in test 6.

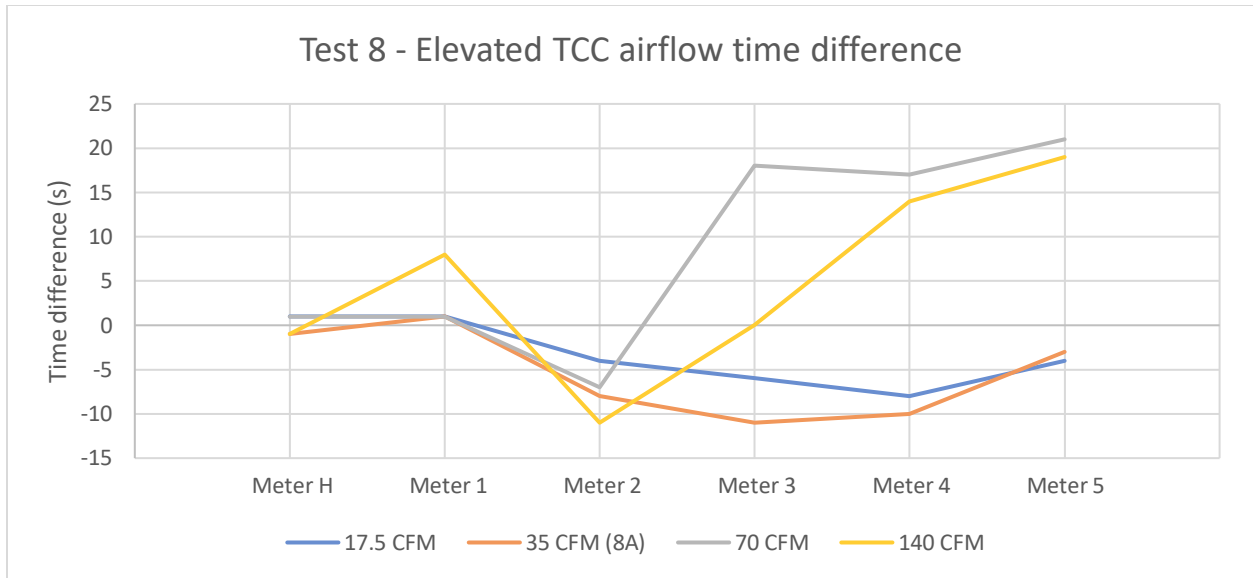


Figure 30: Test 8 varied TCC airflow time difference

Figure 31 shows the time difference from meter 5, which was the most effected meter in most cases. While test 2 and 8 both start with reducing the detection time at low airflow, all of the tests increased the detection time at high airflow. There is no clear indicator how each meter will be affected by TCC airflow, however, after a certain point, increased airflow always increases detection time at all meters past meter 2.

Even though tests 6 and 8 were similar in setup, test 8 consistently had double the time difference as test 6 at meter 5. The curves of their graphs are generally similar as contrasted with tests 2 and 4.

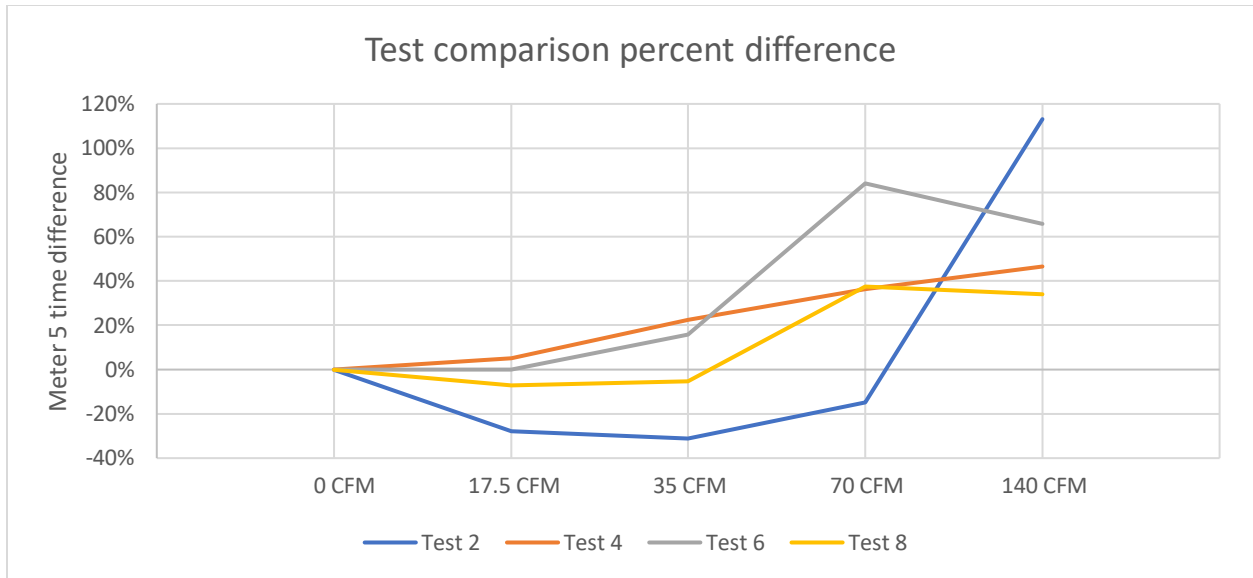


Figure 31: Percent time difference with varied TCC airflow for tests 2, 4, 6, and 8

Conclusion

The simulation results of the smoke tests are an excellent indicator of the usability of Fire Dynamics Simulator as a robust and capable tool for smoke simulation of this scale. Convection was the main driver of airflow in these tests and the simulation was able to match the experimental results with a high degree of accuracy, considering it is a fluid simulation.

Timescale accuracy with a percent error under 7% is an excellent result, giving a high level of confidence in conclusions drawn from the tests. This is the most important metric of accuracy which shows that the convection currents and fluid flow in the simulation was able to match the physical experiments over multiple minutes. The baseline, Test 1, measures an obscuration error of under 20%. The amount of error was consistent in other tests where the same criterion could be used, not all tests had curves that could be compared with the same method.

Using the Envirotainer RKN e1 as a typical TCC, an airflow of 35 CFM was used for the experimental testing. According to the testing and simulations, using TCCs with airflows of 17.5 or 35 CFM has an inconsistent effect on the smoke detection time, at the extremes, ± 20 seconds, $\pm 30\%$ of detection time. At elevated airflow of 70 and 140 CFM, the time to smoke detection almost always increased, an average of 30 seconds (+50%) and at most up to 70 seconds (+110%).

Any amount of airflow produces a measurable change in the smoke detection time. That time difference may be small enough to make no difference in a certification test, or it may be enough to push detection past the 60 second mark for failure in that specific test. There is no predictor of how the smoke detection time will be affected at the lower end of TCC airflow. At double the typical TCC airflow, the smoke detection time will increase. For this reason, it is recommended to keep airflow of TCCs to below 70 CFM.

Future Work

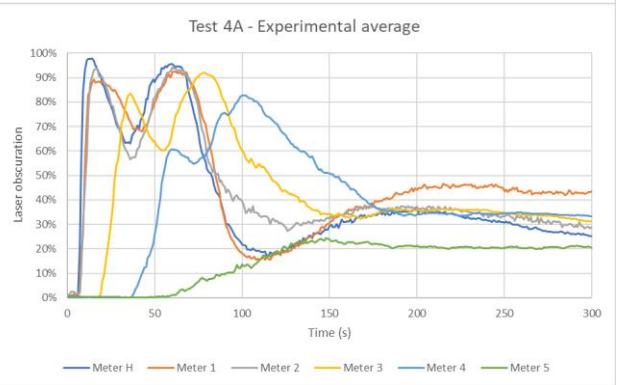
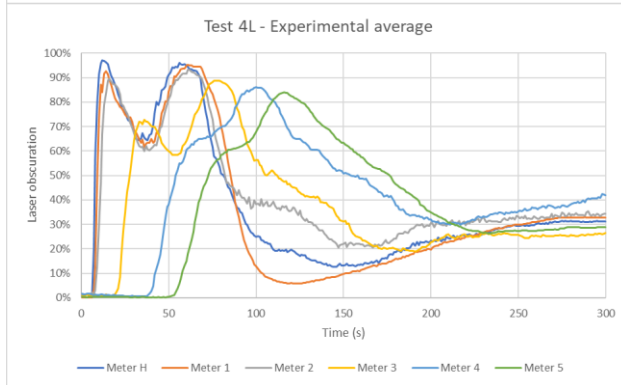
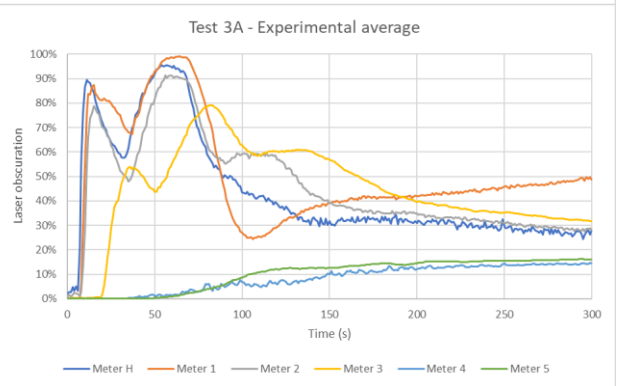
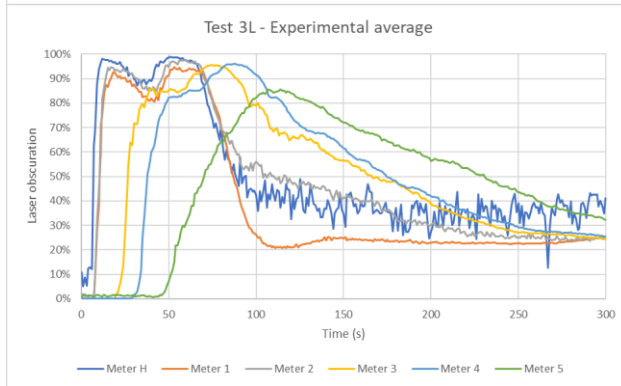
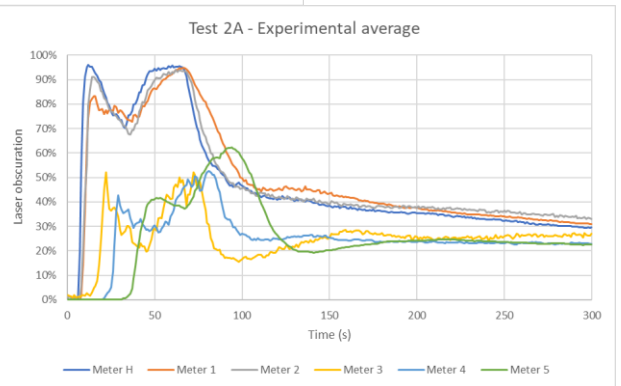
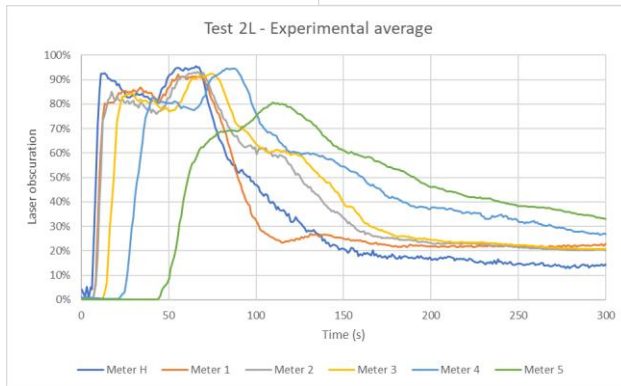
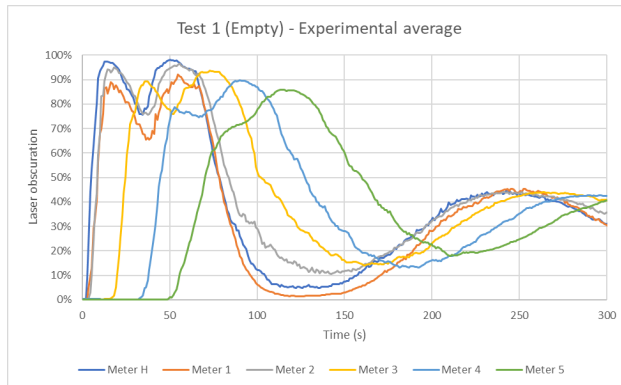
Refinement of the FDS model for the smoke generator should be done with regard for more accurate light scattering and mass extinction coefficient. It may also be possible to tune the characteristics of the particle smoke for better results in longer tests. Care should be taken not to over fit the model, however.

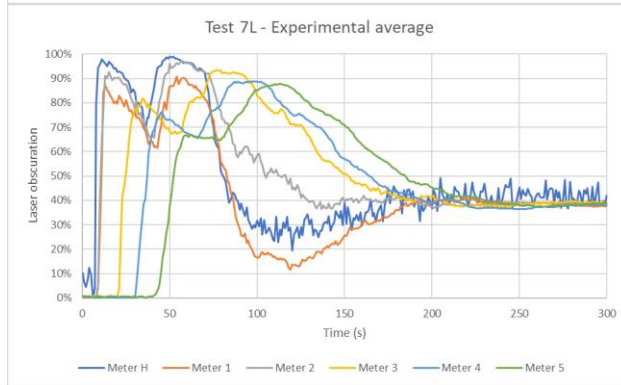
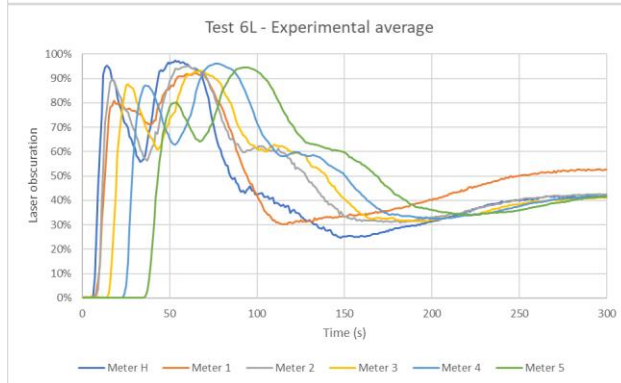
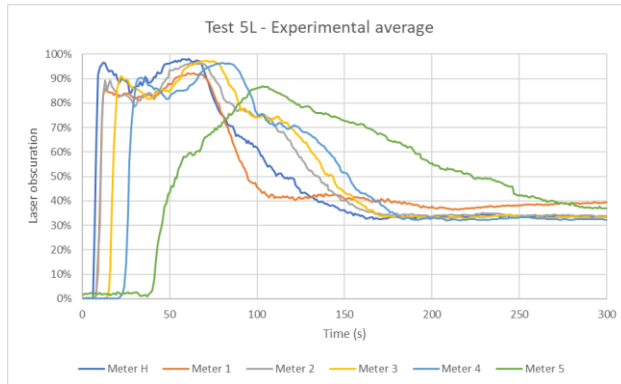
The FDS model can be used in any situation where a smoke generator is needed, provided a controlled test cell. It would be useful for expediting repetitive testing such as evaluating a cargo compartment with every possible configuration of containers. A huge advantage is the

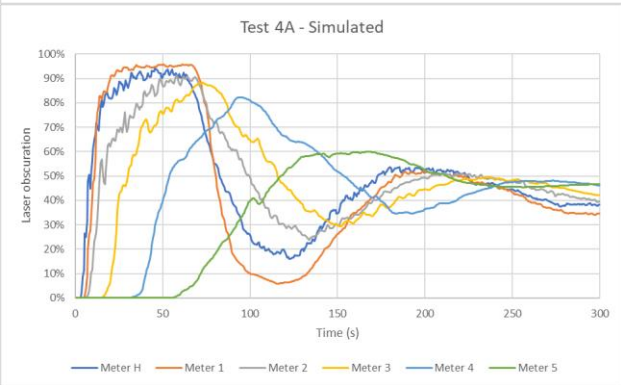
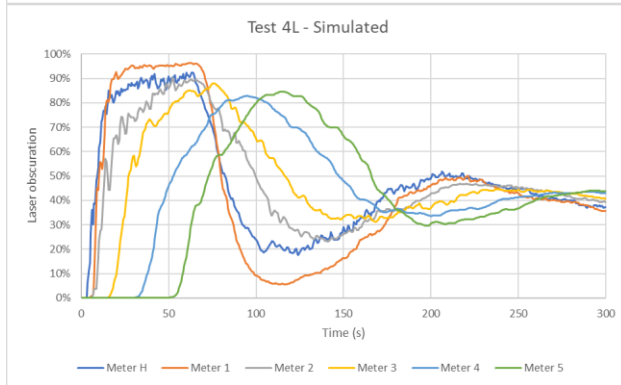
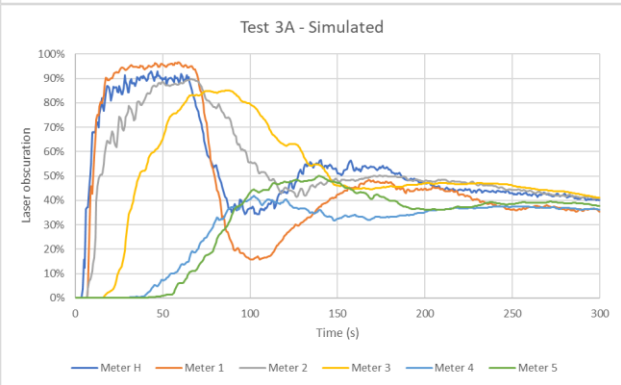
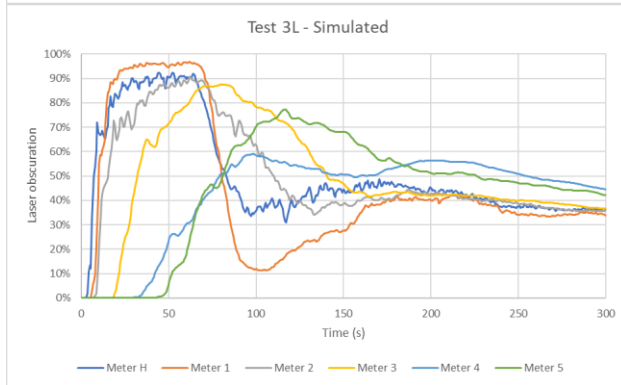
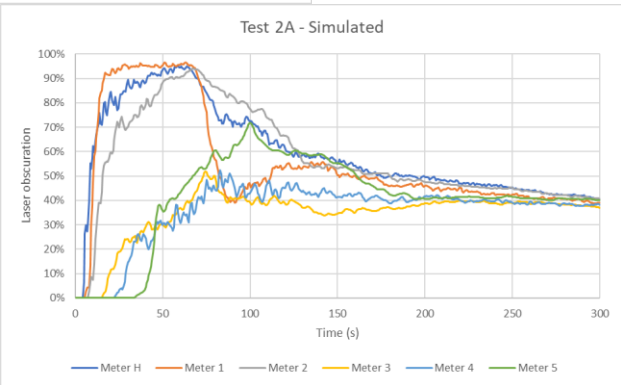
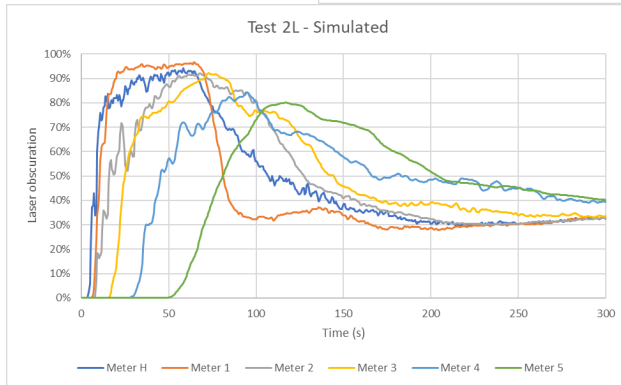
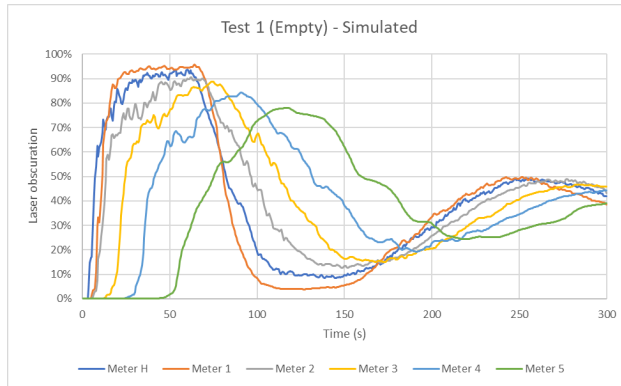
ability to compute the tests in parallel on a server. On average, each test run would take about three hours to compute on the FAA's server. A high-powered personal computer could also run those tests in under 12 hours, depending on the computer's CPU and complexity of the model.

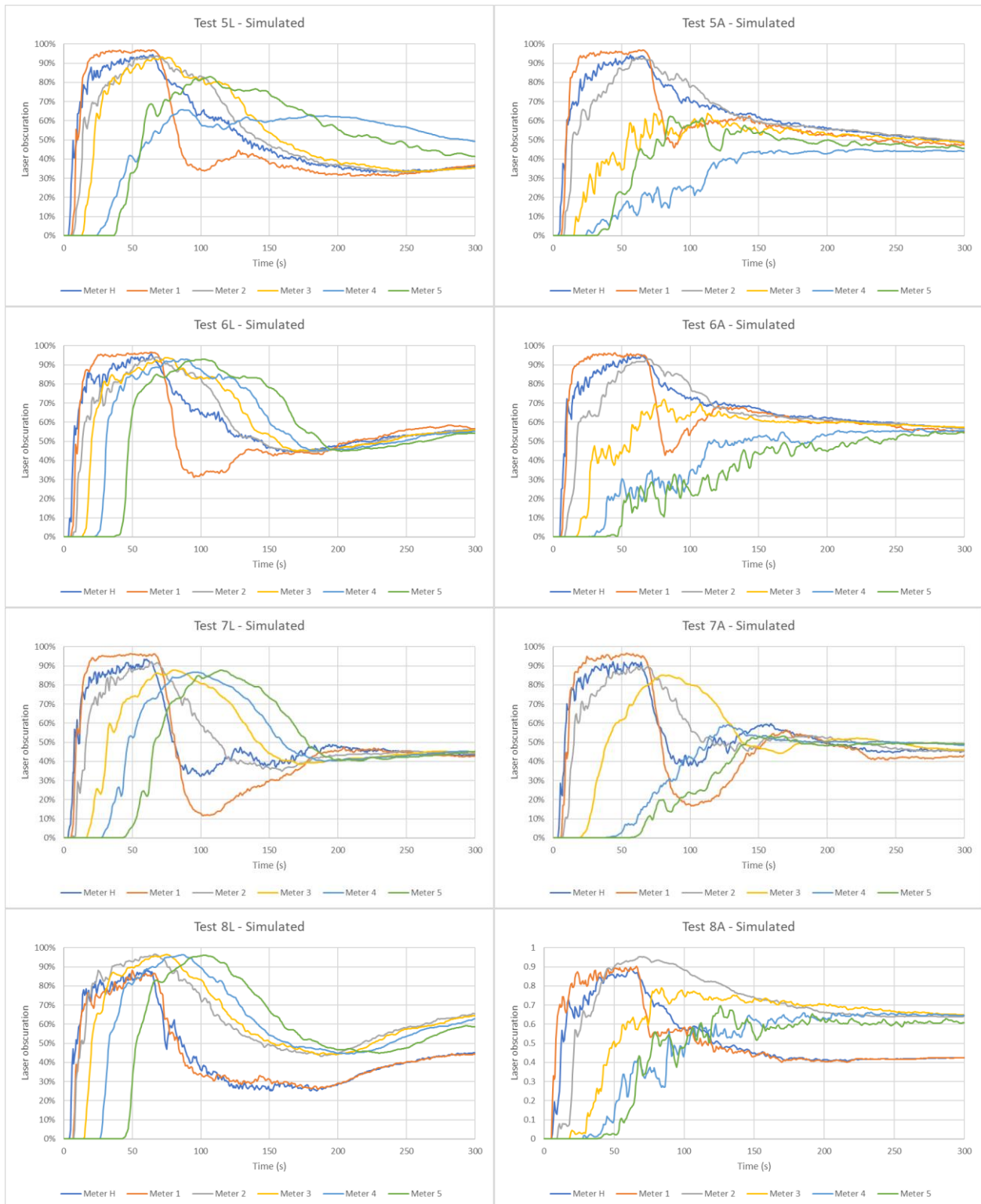
It is possible that future regulation may be written in regard to the maximum airflow or airspeed of exhaust vents in active cargo containers. It would be worth considering the effect of larger exhaust vents with lower airspeed. That study may or may not involve the use of FDS, but this report has shown the accuracy of the FDS model, and it would be wise to utilize the tool.

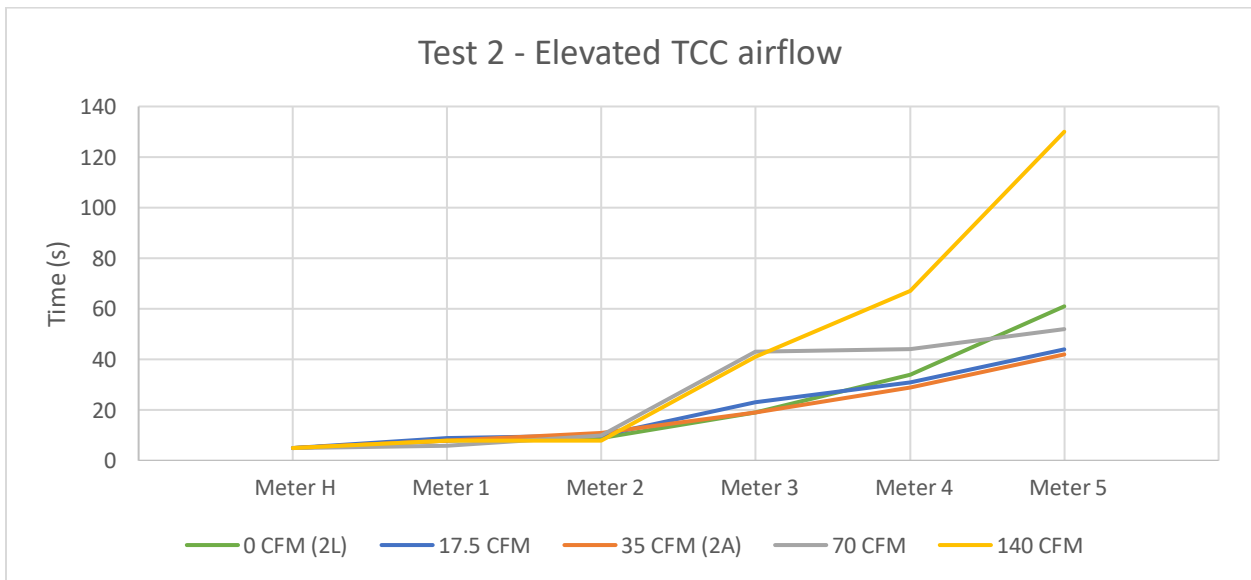
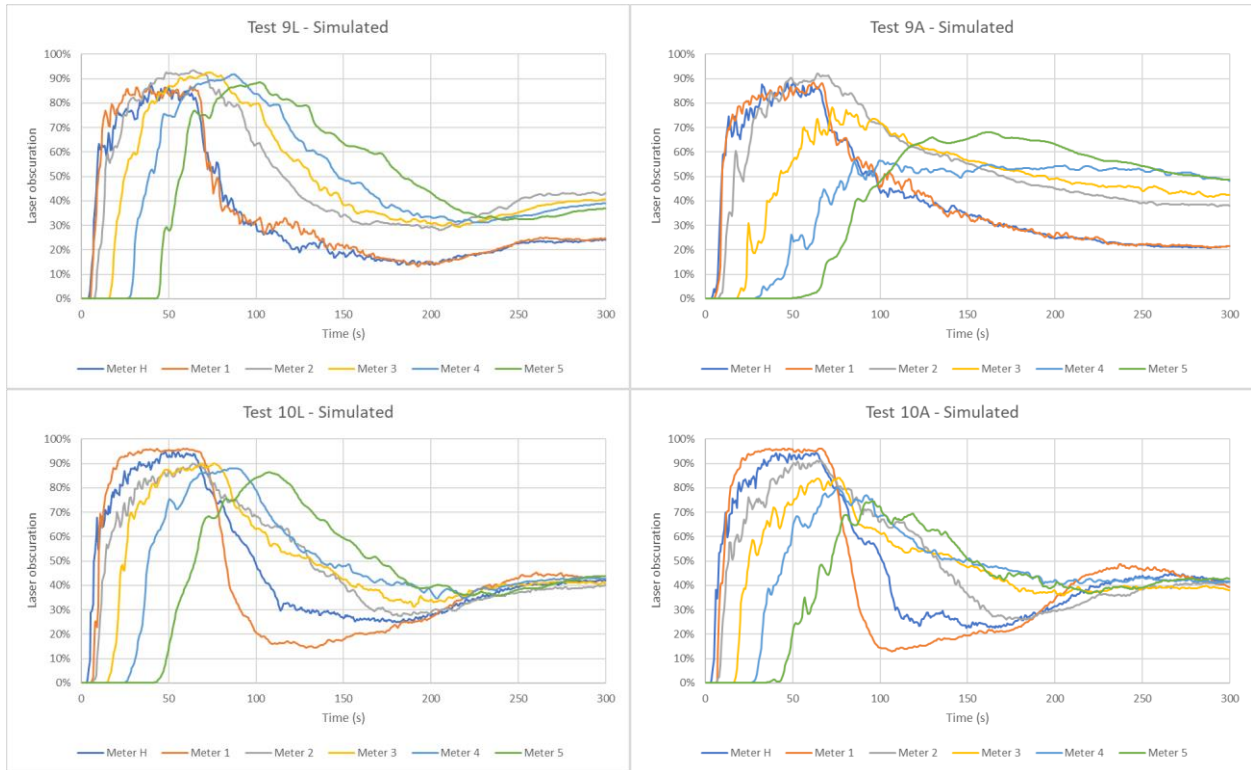
APPENDIX



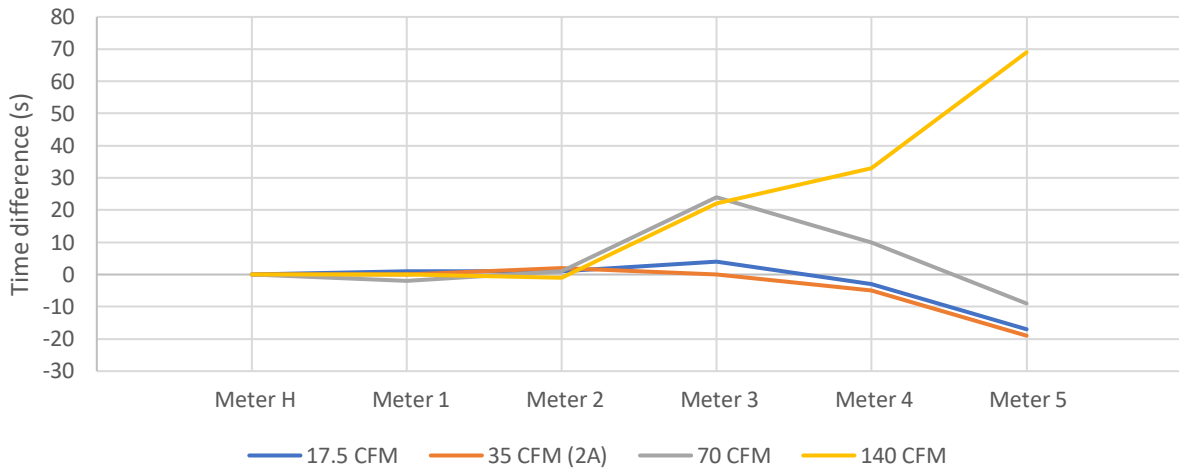




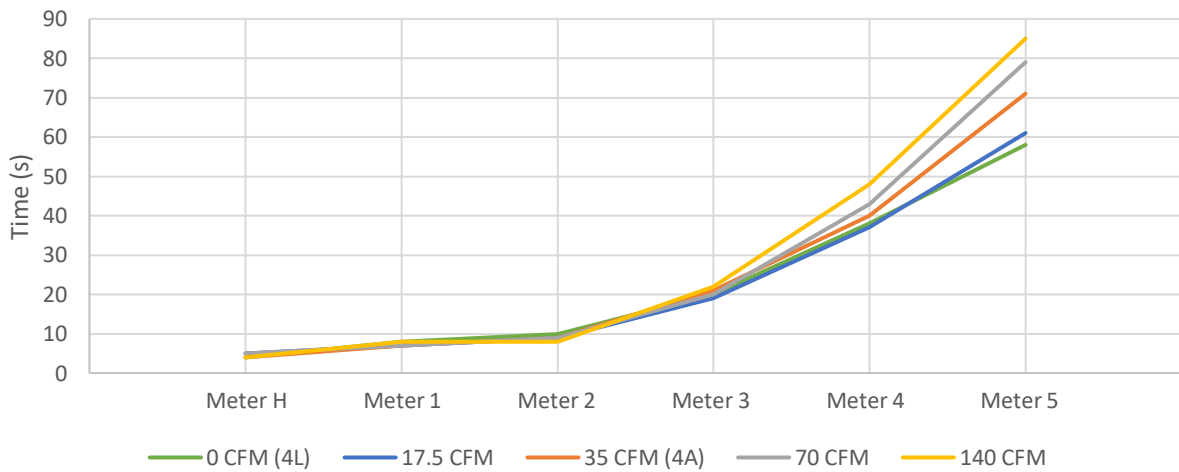




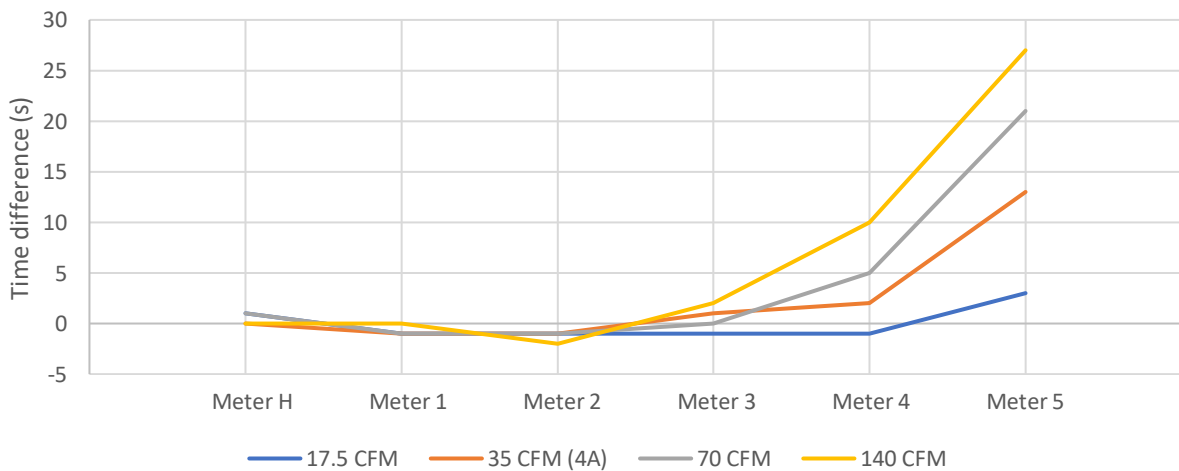
Test 2 - Elevated TCC airflow time difference



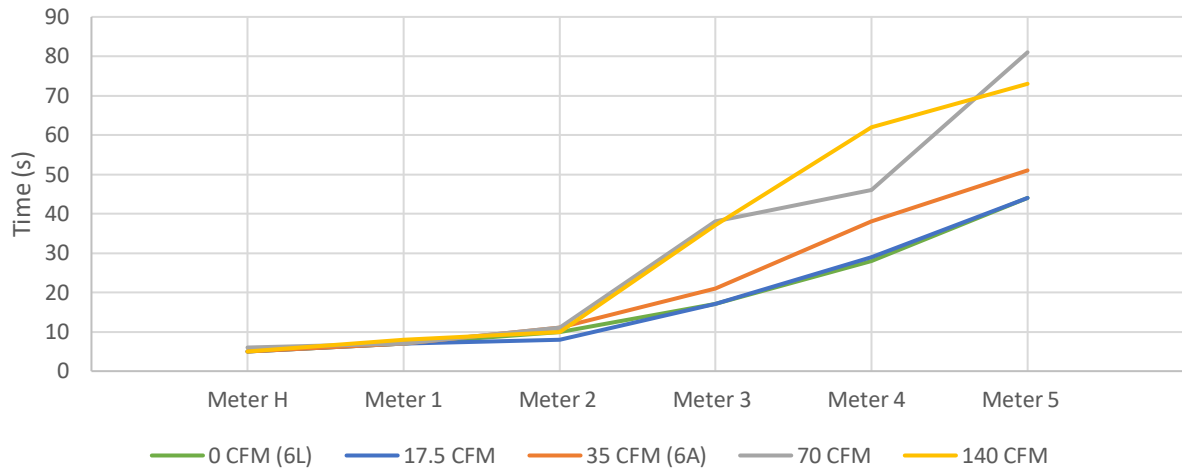
Test 4 - Elevated TCC airflow



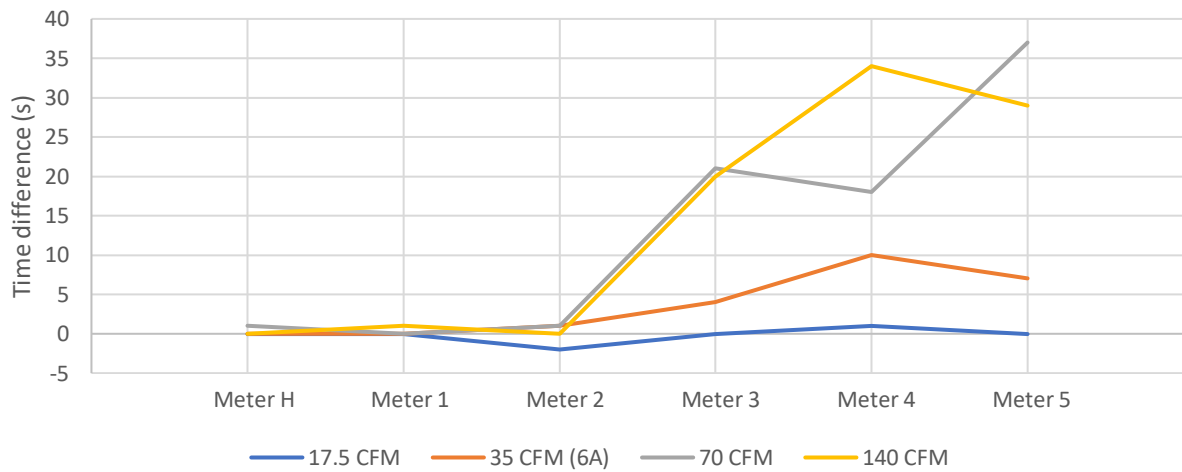
Test 4 - Elevated TCC airflow time difference



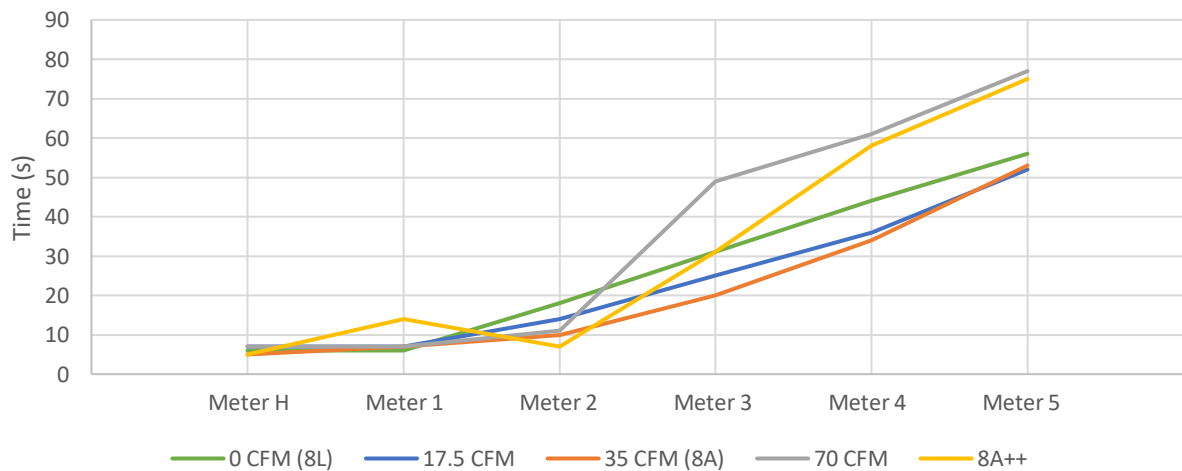
Test 6 - Elevated TCC airflow



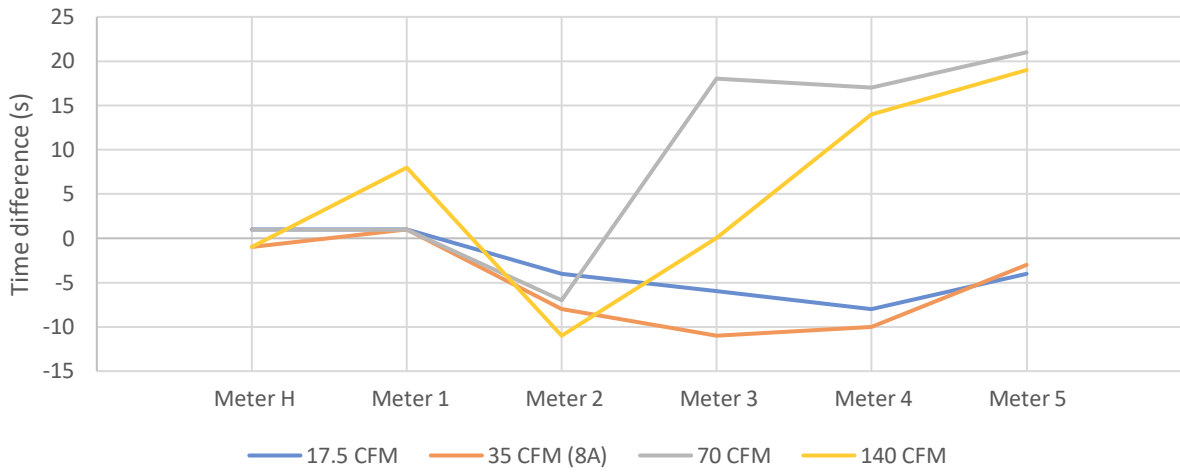
Test 6 - Elevated TCC airflow time difference



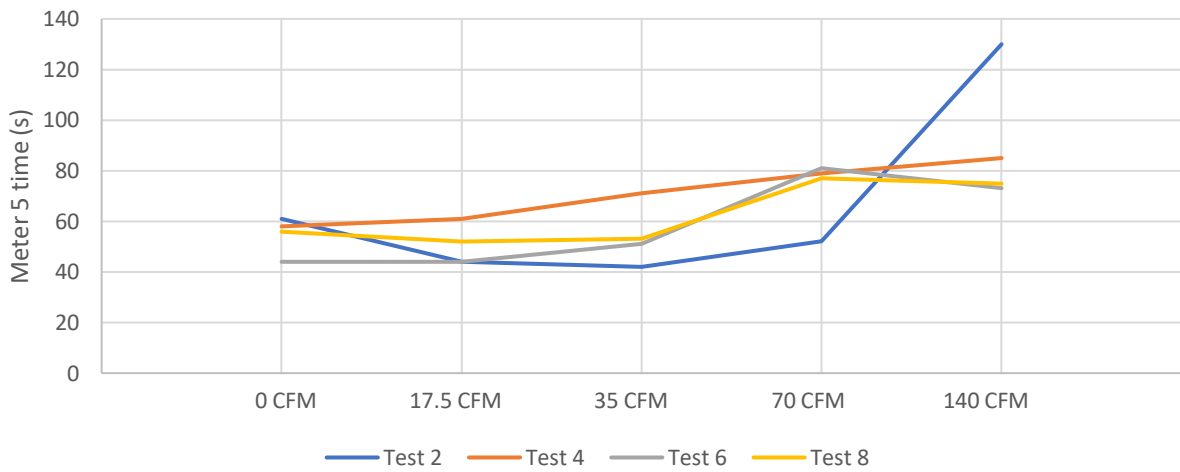
Test 8 - Elevated TCC airflow



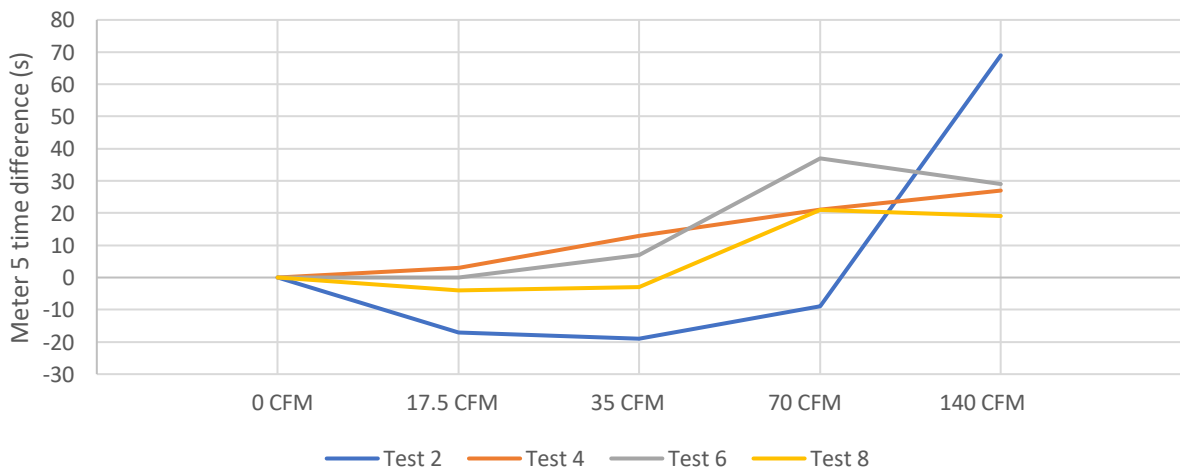
Test 8 - Elevated TCC airflow time difference



Test comparison



Test comparison time difference



REFERENCES

- Blake, D. (2014). *Effects of Cargo Loading and Active Containers on Aircraft Cargo Compartment Smoke Detection Times*. U.S. Department of Transportation, Federal Aviation Administration. Springfield: National Technical Information Service.
- Concept SDT. (n.d.). Retrieved September 2021, from Concept Smoke: https://www.concept-smoke.co.uk/uploads/pdfs/SDT_2016r1.pdf
- Envirotainer. (2021, September 6). RKN e1 Properties. Sweden.
- Karp, M. E. (2019). *Methods for Characterizing Artificial Smoke Generators for Inflight Smoke Detection Certification*. U.S. Department of Transportation, Federal Aviation Administration.
- Meggitt. (2021, February 1). Model 602 Smoke Detector. United Kingdom.
- Ramachadran, S. (2018). Measurements of Aerosols: Instrumentation, Techniques, and Parameters. In *Atmospheric aerosols: Characteristics and radiative effects*. Taylor & Francis Group.
- The Engineering Toolbox*. (2001). Retrieved September 2021, from The Engineering Toolbox: <https://www.engineeringtoolbox.com>

